

Free fermions in disguise without exponential degeneracies

Balázs Pozsgay¹

¹MTA-ELTE “Momentum” Integrable Quantum Dynamics Research Group,
ELTE Eötvös Loránd University, Budapest, Hungary

Abstract

Recently, a number of spin chain models have been discovered that are solvable via hidden free-fermionic structures, going beyond the Jordan-Wigner paradigm. However, all examples in the literature displayed degeneracies that grow exponentially with the volume and that are homogeneous in the spectrum (identical degeneracies for all energy levels). In this note we present a model that can be solved by “free fermions in disguise” (FFD), such that the spectrum is free from exponential degeneracies for generic coupling constants. The model can be seen as a particular perturbation of two Ising chains. Alternatively, it can be realized as an interpolation between a standard Jordan-Wigner solvable chain and the original FFD model of Fendley. We used ChatGPT Pro 5.4 and 5.5 as a research assistant; in the Supplemental Material we provide details about the collaboration between the AI and the human author.

1 Introduction

Finding exactly solvable models is of continuing interest in quantum many-body physics, or theoretical physics more generally. Arguably the simplest models are those that can be solved by free bosons or free fermions. In certain cases a model Hamiltonian can appear to be interacting; nevertheless it can be brought into a quadratic form in free variables/operators by using an appropriate transformation.

In quantum spin chains the most famous example for such an operation is the Jordan-Wigner transformation [1], which introduces Dirac or Majorana fermions acting on the Hilbert space of the spin-1/2 chain. The Jordan-Wigner transformation has a canonical form that is used routinely to treat, for example, the quantum Ising chain or the XY models, but it also has various algebraic generalizations (see, for example, [2, 3, 4]). The conditions for generalized Jordan-Wigner solvability were determined recently in the independent works [5, 6].

In a seminal work [7] Fendley discovered a spin chain model that was shown to be free-fermionic, although its solution does not fit into the Jordan-Wigner framework. The title of the paper was “free fermions in disguise” (FFD), and this name was subsequently used in several follow-up papers to denote the model or families of such models. The methods of [7] were soon generalized to similar models in [8], where it was also shown that the FFD model cannot be solved by a generalized Jordan-Wigner transformation. In this work we do not attempt to review the literature on the FFD model and its various generalizations; instead we refer the reader to a recent work [9] where an in-depth review is given.

We instead focus on a particular problem that has so far plagued all FFD-type models: the exponential degeneracies in the spectrum. It was already recognized in [7] that in the FFD model the number of free-fermionic eigenmodes is far less than the number of qubits on which the model is

defined. As a result, every energy level is degenerate, so that the degeneracy is homogeneous along the spectrum. The number of fermionic eigenmodes typically grows linearly with the length of the spin chain, but with a coefficient smaller than 1. As a result, there will be an extensive number of zero modes that generate a very non-trivial symmetry algebra [7, 10]. These zero modes are responsible for the exponential degeneracies.

Based on the seminal works it appeared that such exponential degeneracies are inevitable. The technical reason for the missing eigenmodes can be formulated using algebra and graph theory [8] (see also [11] and Subsection 4.2 below). It is notable that exponential degeneracies were present even in those models [12, 13] whose construction evaded some of the limitations presented in [8]. However, no compelling physical argument was known as to why it has to be this way.

In this work we present an FFD-type model that is free from exponential degeneracies (for generic coupling constants). In other words, the number of fermionic eigenmodes in the model is either equal to the number of qubits in the chain, or the difference is only $\mathcal{O}(1)$. We present the model in an abstract algebraic formulation, but we also provide two representations. The first one is via two coupled quantum Ising chains. The second representation can be seen as an interpolation between the XY chain (given by the Dzyaloshinskii–Moriya interaction term) and the original FFD model of Fendley.

This interpolation is one of the key results of our work. It shows that the FFD-type models and the Jordan-Wigner solvable ones are not truly separate families. Instead, the Jordan-Wigner solvable models are simply very special examples in the wide family of free-fermionic models. This point of view was already advocated in [14] and more recently in [11, 9]. However, to our knowledge the present model is the first one that allows for a continuous transition between these apparently different families.

Our final Hamiltonians are linear combinations of two Hamiltonians, each of which is free-fermionic, and their algebraic structures are compatible with each other. A single Hamiltonian only has half the number of eigenmodes needed, but the linear combination of the two Hamiltonians finally leads to a spectrum that is generally non-degenerate or has a homogeneous degeneracy of 2 or 4. The mechanism for the mutual commutativity of the algebraic structures is very similar to the mechanism that underlies the free-fermionic solvability of the model of [12]. A crucial difference is that in the model of [12] there was just one Hamiltonian (with half the number of eigenmodes needed) and there was no obvious way to introduce a second, complementary Hamiltonian.

In the next section we introduce the abstract algebra behind our model and we give two concrete representations. Then, in Subsection 2.5, we collect the key results and give a map to this paper. Our conclusions are presented in Section 8 together with some open problems.

The use of AI in this work.

We used ChatGPT 5.4 and 5.5 Pro as a research assistant. Most computations were performed by the AI, and were checked later by the human author. Besides analytic checks, we also performed a numerical test: an exact diagonalization routine was programmed and run by the human author, completely independently of the numerical work of the AI. We found agreement with the numerical results of the AI and we independently confirmed the free-fermionic spectrum for generic coupling constants.

The text was written in a collaboration between the human and the AI. The Abstract, the Introduction, and the Conclusions were written exclusively by the human author.

It may be of interest to spell out what the actual substantial contributions of the AI were and which points required the insight of the human author. We present a list of these points in a Supplemental Material¹.

¹It can be downloaded as a separate PDF file from the preprint server.

2 The model and the main results

2.1 The Ising algebra and the Hamiltonians

We define our models via an abstract algebra. This algebra is a double tensor product of two identical Ising-type algebras. We now give the precise definitions.

Fix an integer $M \geq 2$. We have two families of generators B_j and \tilde{B}_j with M elements each, satisfying

$$B_j = B_j^\dagger, \quad \tilde{B}_j = \tilde{B}_j^\dagger, \quad j = 1, \dots, M. \quad (2.1)$$

Their squares are proportional to the identity:

$$B_j^2 = \beta_j^2 \mathbf{1}, \quad \tilde{B}_j^2 = \tilde{\beta}_j^2 \mathbf{1}. \quad (2.2)$$

Here β_j and $\tilde{\beta}_j$ are real non-zero parameters.

The two families of generators satisfy the same algebra:

$$\{B_j, B_{j+1}\} = 0, \quad [B_j, B_k] = 0 \quad (|j - k| > 1), \quad (2.3)$$

$$\{\tilde{B}_j, \tilde{B}_{j+1}\} = 0, \quad [\tilde{B}_j, \tilde{B}_k] = 0 \quad (|j - k| > 1). \quad (2.4)$$

It is important that there is no periodicity assumed. Thus each family is an open Ising-type algebra. The two families commute with one another:

$$[B_j, \tilde{B}_k] = 0 \quad \text{for all } j, k. \quad (2.5)$$

We also introduce special cubic products, which couple the two algebras:

$$A_j := i\lambda_j B_j B_{j+1} \tilde{B}_j, \quad \tilde{A}_j := -i\tilde{\lambda}_j \tilde{B}_j \tilde{B}_{j+1} B_{j+1}, \quad (j = 1, \dots, M - 1), \quad (2.6)$$

where $\lambda_j, \tilde{\lambda}_j \in \mathbb{R}$ and we assume again that all of them are non-zero. The factors i and $-i$ make these operators Hermitian, because $B_j B_{j+1}$ and $\tilde{B}_j \tilde{B}_{j+1}$ are anti-Hermitian. The squares of A_j and \tilde{A}_j are also scalar. We write

$$A_j^2 = \alpha_j^2 \mathbf{1}, \quad \tilde{A}_j^2 = \tilde{\alpha}_j^2 \mathbf{1}, \quad (2.7)$$

where we introduced

$$\alpha_j = \lambda_j \beta_j \beta_{j+1} \tilde{\beta}_j, \quad \tilde{\alpha}_j = \tilde{\lambda}_j \tilde{\beta}_j \tilde{\beta}_{j+1} \beta_{j+1}. \quad (2.8)$$

We define two Hamiltonians

$$H_1 = \sum_{j=1}^M B_j + \sum_{j=1}^{M-1} A_j, \quad H_2 = \sum_{j=1}^M \tilde{B}_j + \sum_{j=1}^{M-1} \tilde{A}_j. \quad (2.9)$$

As final Hamiltonians we will consider the combinations $H_1 \pm H_2$.

The most important case of the final Hamiltonian is obtained when all cubic coefficients collapse to one global parameter,

$$\lambda_j = \tilde{\lambda}_j = \lambda \quad (j = 1, \dots, M - 1). \quad (2.10)$$

Then

$$A_j = i\lambda B_j B_{j+1} \tilde{B}_j, \quad \tilde{A}_j = -i\lambda \tilde{B}_j \tilde{B}_{j+1} B_{j+1}. \quad (2.11)$$

In this case the model has $2M + 1$ free parameters, given by the Ising-type couplings $\beta_j, \tilde{\beta}_j$ and the global parameter λ . We could remove an overall normalization factor (for example by setting $\lambda = 1$). However, it is convenient to keep these parameters at the moment.

2.2 Frustration graphs and simplicial cliques

The notion of a frustration graph will be used repeatedly below. Frustration graphs can be introduced for sets of Pauli strings (products of Pauli matrices acting on the Hilbert space of a lattice spin model). A Pauli string always squares to ± 1 , and two Pauli strings either commute or anti-commute. The commutation rules can be encoded conveniently by a graph: we draw a vertex for each Pauli string, and for a pair of Pauli strings we draw an edge if and only if they anti-commute.

These algebraic properties can be generalized to a more abstract setting, opening the way to “graph-Clifford algebras” [15, 11]. Let us assume that we are dealing with an abstract algebra, where every generator squares to the identity, and two generators either commute or anti-commute. Then we encode these properties into the frustration graph in the same way as for the concrete Pauli strings: We draw vertices for the generators, and we connect two vertices if and only if the two generators anti-commute. As an illustration, a frustration graph corresponding to the algebra of one family of the B_j operators is shown in Figure 1.

Frustration graphs play a central role in establishing the free-fermionic properties (and more generally: integrability) in the lattice models that we study.

In the original definition of graph-Clifford algebras the generators are algebraically independent of each other. However, the frustration graph can be introduced even in those cases when there are relations between the generators. The effects of the extra relations will be discussed below. If we treat the terms in H_1 and H_2 as independent, then the frustration graphs for both Hamiltonians are as shown in Fig. 2.



Figure 1: Frustration graph for one copy of the Ising-type algebra for $M = 6$.

2.3 Representation by coupled Ising chains

A faithful local representation of the two commuting Ising algebras is obtained on two auxiliary Ising chains with Pauli operators σ_r^α and τ_r^α :

$$B_{2r-1} \mapsto \beta_{2r-1} \sigma_r^z, \quad B_{2r} \mapsto \beta_{2r} \sigma_r^x \sigma_{r+1}^x. \quad (2.12)$$

$$\tilde{B}_{2r-1} \mapsto \tilde{\beta}_{2r-1} \tau_r^z, \quad \tilde{B}_{2r} \mapsto \tilde{\beta}_{2r} \tau_r^x \tau_{r+1}^x. \quad (2.13)$$

The auxiliary length may be chosen as $\lceil (M+1)/2 \rceil$. Each Ising algebra is represented by the usual alternating field/bond algebra of an open Ising chain.

The cubic products then give the three-site generators

$$A_{2r-1} \mapsto -\alpha_{2r-1} \sigma_r^y \sigma_{r+1}^x \tau_r^z, \quad A_{2r} \mapsto \alpha_{2r} \sigma_r^x \sigma_{r+1}^y \tau_r^x \tau_{r+1}^x, \quad (2.14)$$

$$\tilde{A}_{2r-1} \mapsto \tilde{\alpha}_{2r-1} \sigma_r^x \sigma_{r+1}^x \tau_r^y \tau_{r+1}^x, \quad \tilde{A}_{2r} \mapsto -\tilde{\alpha}_{2r} \sigma_{r+1}^z \tau_r^x \tau_{r+1}^y. \quad (2.15)$$

Thus the algebraic Hamiltonian is represented as a local two-leg Ising ladder with open boundary conditions. The total number of qubits used in the construction is $2\lceil (M+1)/2 \rceil$.

2.4 Representation from the FFD perturbation of an XY chain

We now use the alternative notation X_j, Y_j, Z_j for the Pauli matrices acting on site j . The algebra above has the following realization on a spin chain of length $L = M + 1$:

$$B_j = \beta_j Y_j X_{j+1}, \quad \tilde{B}_j = \tilde{\beta}_j X_j Y_{j+1}, \quad (2.16)$$

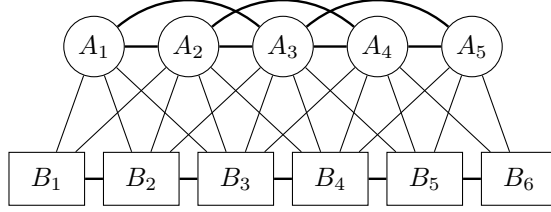


Figure 2: Frustration graph for the Hamiltonian H_1 for $M = 6$. The terms A_k are algebraically dependent on the generators B_j and \tilde{B}_j ; however, if we focus on H_1 alone, then we can regard them as independent operators, and thus the corresponding independent vertices are added to the graph. The Hamiltonian H_2 has an identical frustration graph.

and

$$A_j = \alpha_j Z_j X_{j+1} X_{j+2}, \quad \tilde{A}_j = \tilde{\alpha}_j X_j X_{j+1} Z_{j+2}. \quad (2.17)$$

It is worthwhile to consider the antisymmetric combination $H_1 - H_2$. Focusing on the homogeneous version, where we set $\beta_j = \tilde{\beta}_j = 1$ and $\lambda_j = \tilde{\lambda}_j = \lambda$, we get

$$H_1 - H_2 = \sum_{j=1}^{L-1} (Y_j X_{j+1} - X_j Y_{j+1}) + \lambda \sum_{j=1}^{L-2} (Z_j X_{j+1} X_{j+2} - X_j X_{j+1} Z_{j+2}). \quad (2.18)$$

Here the nearest-neighbour part is a Jordan-Wigner solvable, $U(1)$ -symmetric XY chain. More precisely, it is given by the Dzyaloshinskii–Moriya interaction term, which can be transformed to the standard form by a homogeneous twist transformation. The three-site interaction in the Hamiltonian above is the antisymmetric combination of the terms found in Fendley’s free-fermion-in-disguise construction [7].

We note that the two representations have the same qubit count for odd M , whereas for even M the Ising representation has one more qubit than the XY representation.

2.5 Main results

This article proves the following statements for the Hamiltonians $H_{1,2}$ without using either concrete representation in the proofs.

- (i) The local cross-relations of the cubic algebra imply a complete commutativity criterion. Namely, we find the commutativity $[H_1, H_2] = 0$ if and only if

$$\lambda_j = \tilde{\lambda}_j = \lambda_{j+1}, \quad (2.19)$$

for all indices for which the equation is defined. Hence the generic commuting family is the global- λ family (2.11). This is shown in Section 3.

We stress that the terms in H_1 and H_2 do not all commute with one another, and the special algebraic properties are needed for the cancellations.

- (ii) Each Hamiltonian is separately free-fermionic: their frustration graphs are even-hole-free and claw-free, so the free-fermion machinery of [8, 11] applies. More specifically, we can diagonalize the Hamiltonians as

$$H_1 = \sum_{k=1}^S \varepsilon_{1,k} \mathcal{Z}_{1,k}, \quad H_2 = \sum_{k=1}^S \varepsilon_{2,k} \mathcal{Z}_{2,k}, \quad (2.20)$$

where $\mathcal{S} = \lfloor (M + 1)/2 \rfloor$ is the number of fermionic eigenmodes, $\varepsilon_{a,k}$ with $a = 1, 2$ and $k = 1, \dots, \mathcal{S}$ are the single-particle energies, and $\mathcal{Z}_{a,k}$ are mode occupation operators with the properties

$$\mathcal{Z}_{a,k}^2 = 1, \quad [\mathcal{Z}_{a,k}, \mathcal{Z}_{a,\ell}] = 0. \quad (2.21)$$

These operators are constructed from fermionic ladder operators $\Psi_{a,\pm k}$ as

$$\mathcal{Z}_{a,k} = [\Psi_{a,k}, \Psi_{a,-k}]. \quad (2.22)$$

The ladder operators satisfy the canonical anti-commutation algebra, which in our convention reads

$$\{\Psi_{a,k}, \Psi_{a,\ell}\} = \delta_{k+\ell}. \quad (2.23)$$

We also construct transfer matrices $T_{1,M}(u)$ and $T_{2,M}(u)$ satisfying

$$[T_{1,M}(u), T_{1,M}(v)] = 0, \quad [T_{2,M}(u), T_{2,M}(v)] = 0. \quad (2.24)$$

This is discussed in Section 4.

- (iii) The free-fermionic structures of the two Hamiltonians are also mutually commutative:

$$[\mathcal{Z}_{1,k}, \mathcal{Z}_{2,\ell}] = 0. \quad (2.25)$$

This is established using the commutativity of H_1 and H_2 and their free-fermionic decomposition. Furthermore, we prove the cross-commutativity of the transfer matrices

$$[T_{1,M}(u), T_{2,M}(v)] = 0. \quad (2.26)$$

The proofs are presented in Subsection 5.1.

- (iv) We also treat the compatibility of the ladder operators. After adjoining compatible edge operators, the two hidden Dirac families can be chosen either mutually commuting or mutually anti-commuting. This is presented in Subsection 5.2.
- (v) In the spatially homogeneous case, the one-particle energies are encoded by an explicit scalar polynomial. We find the explicit recursion relation for this polynomial and study the large-volume limits. This leads to standing-wave equations for the single-particle modes. In two special limits we obtain the one-particle energies of the Ising model and the FFD model, respectively. This is presented in Section 7.

In Section 6 we discuss the degeneracies of the spectra in these models. The actual degeneracies depend on the representation chosen. The final statement for generic couplings is as follows: If M is odd, then all energy levels are non-degenerate in both representations. If M is even, then there is a homogeneous degeneracy of 4 in the Ising representation and 2 in the XY representation. Numerical data for the XY case is presented in Appendix A.

In two further appendices we present two computations that are not crucial for our main line of argument, but further support the claim that our model is indeed a natural extension of Fendley's FFD model:

- (i) The highly non-local transfer matrices can be factorized into a product of local operators, similar to the factorization derived earlier in [7] (see also [16]). This is presented in Appendix B.

- (ii) The transfer matrices and the fermionic operators can be expressed as Matrix Product Operators (MPOs) with fixed small bond dimension. We treat only the XY representation. In that representation the transfer matrix admits an MPO representation with bond dimension 3, so that this MPO is a simple modification of the one found by Fendley [7]. The fermionic operators can be represented as an inhomogeneous MPO of bond dimension 4. This appears to be a new result even for the original FFD model. These computations are presented in Appendix C.

3 Local algebra and mutual commutativity

Here we investigate the commutation relations between the terms in the Hamiltonians H_1 and H_2 . We determine the frustration graphs that we would obtain if the A_k and \tilde{A}_k operators were algebraically independent generators. We also establish the sufficient and necessary condition for the global commutativity of H_1 and H_2 .

3.1 Same-family relations and frustration graphs

The definitions (2.6) determine all the commutation relations inside a single Hamiltonian.

Lemma 3.1 (Internal sign rules). *In the H_1 family, the only anti-commuting pairs are*

$$\{B_j, B_k\} = 0 \iff |j - k| = 1, \quad (3.1)$$

$$\{A_j, B_k\} = 0 \iff k \in \{j - 1, j, j + 1, j + 2\}, \quad (3.2)$$

$$\{A_j, A_k\} = 0 \iff 1 \leq |j - k| \leq 2. \quad (3.3)$$

All other same-family pairs commute. The same statements hold for the tilded family.

Proof. Only the Ising-algebra signs are used. The relation for B_j, B_k is one of the defining relations. Since $A_j = i\lambda_j B_j B_{j+1} \tilde{B}_j$ and all B 's commute with all \tilde{B} 's, commuting B_k through A_j only counts the signs produced by $B_j B_{j+1}$. There is one such sign exactly for $k \in \{j - 1, j, j + 1, j + 2\}$, which proves (3.2).

For A_j and A_k , the B -part contributes the parity of the adjacent crossings between the two sets $\{j, j + 1\}$ and $\{k, k + 1\}$, while the \tilde{B} -part contributes the parity of the crossing between \tilde{B}_j and \tilde{B}_k . The total parity is odd exactly when the intervals $[j, j + 2]$ and $[k, k + 2]$ overlap without being identical, i.e. when $1 \leq |j - k| \leq 2$. This proves (3.3). The tilded case is identical with the two Ising chains exchanged. \square

From these relations we can draw the frustration graphs. We obtain examples for the so-called interval graphs. An interval graph is defined as follows: vertices correspond to intervals on the real line, and we draw edges between two vertices if the corresponding two intervals overlap. Let us now introduce the following intervals for the generators in H_1 :

$$I(B_j) = [j, j + 1], \quad I(A_j) = [j, j + 2]. \quad (3.4)$$

We can see that the frustration graph of H_1 is the interval graph of the intervals (3.4). The same graph governs H_2 . As an illustration, see Figure 2, which depicts the graph for $M = 6$.

In a later section, an important role will be played by the so-called independence number of the graphs, which is defined as the maximal size of a subset of the vertices such that no two vertices are connected. It is easy to see that in these graphs the independence number is $\mathcal{S} = \lfloor \frac{M+1}{2} \rfloor$.

3.2 Cross-relations and commutativity criterion

We now list the commutation relations between the terms in the two different Hamiltonians.

Lemma 3.2 (Algebraic cross-relations). *For all allowed indices,*

$$[B_j, \tilde{B}_k] = 0, \quad [A_j, \tilde{A}_k] = 0. \quad (3.5)$$

The only mixed anti-commuting pairs are

$$\{A_j, \tilde{B}_{j-1}\} = 0, \quad \{A_j, \tilde{B}_{j+1}\} = 0, \quad \{B_j, \tilde{A}_j\} = 0, \quad \{B_{j+2}, \tilde{A}_j\} = 0. \quad (3.6)$$

Moreover, the paired products have the following common normal forms:

$$A_j \tilde{B}_{j+1} = i\lambda_j B_j B_{j+1} \tilde{B}_j \tilde{B}_{j+1}, \quad B_j \tilde{A}_j = -i\tilde{\lambda}_j B_j B_{j+1} \tilde{B}_j \tilde{B}_{j+1}, \quad (3.7)$$

$$A_{j+1} \tilde{B}_j = -i\lambda_{j+1} B_{j+1} B_{j+2} \tilde{B}_j \tilde{B}_{j+1}, \quad B_{j+2} \tilde{A}_j = i\tilde{\lambda}_j B_{j+1} B_{j+2} \tilde{B}_j \tilde{B}_{j+1}. \quad (3.8)$$

In the global- λ family these imply the exact square identities

$$A_j \tilde{B}_{j+1} = -B_j \tilde{A}_j, \quad A_{j+1} \tilde{B}_j = -B_{j+2} \tilde{A}_j. \quad (3.9)$$

Proof. The relation $[B_j, \tilde{B}_k] = 0$ is part of the defining algebra. For $[A_j, \tilde{A}_k]$, move the B -part $B_j B_{j+1}$ through the single B -factor B_{k+1} in \tilde{A}_k , and move the single \tilde{B} -factor \tilde{B}_j through the \tilde{B} -part $\tilde{B}_k \tilde{B}_{k+1}$. The two parities agree for every j, k : for $k = j - 2, j - 1, j, j + 1$ both parities are odd, and otherwise both are even. Hence the total parity is always even.

The list (3.6) follows by the same sign count. For example, A_j contains one tilded factor, namely \tilde{B}_j , so it anti-commutes with \tilde{B}_k precisely when $k = j \pm 1$. Similarly, \tilde{A}_j contains the single untilded factor B_{j+1} , so it anti-commutes with B_k precisely when $k = j$ or $k = j + 2$.

Finally, putting the paired products into the same normal order gives

$$A_j \tilde{B}_{j+1} = i\lambda_j B_j B_{j+1} \tilde{B}_j \tilde{B}_{j+1}, \quad (3.10)$$

$$B_j \tilde{A}_j = -i\tilde{\lambda}_j B_j \tilde{B}_j \tilde{B}_{j+1} B_{j+1} = -i\tilde{\lambda}_j B_j B_{j+1} \tilde{B}_j \tilde{B}_{j+1}, \quad (3.11)$$

which proves (3.7). Likewise,

$$A_{j+1} \tilde{B}_j = i\lambda_{j+1} B_{j+1} B_{j+2} \tilde{B}_{j+1} \tilde{B}_j = -i\lambda_{j+1} B_{j+1} B_{j+2} \tilde{B}_j \tilde{B}_{j+1}, \quad (3.12)$$

$$B_{j+2} \tilde{A}_j = -i\tilde{\lambda}_j B_{j+2} \tilde{B}_j \tilde{B}_{j+1} B_{j+1} = i\tilde{\lambda}_j B_{j+1} B_{j+2} \tilde{B}_j \tilde{B}_{j+1}, \quad (3.13)$$

which proves (3.8). \square

As an application we have the following:

Theorem 3.3 (Algebraic mutual commutativity). *We have*

$$[H_1, H_2] = 0 \quad (3.14)$$

if and only if

$$\lambda_j = \tilde{\lambda}_j \quad (1 \leq j \leq M - 1) \quad (3.15)$$

and

$$\lambda_{j+1} = \tilde{\lambda}_j \quad (1 \leq j \leq M - 2). \quad (3.16)$$

Equivalently, all local coefficients are equal to one global parameter λ .

Proof. By Lemma 3.2, the only non-zero mixed commutators are the four families in (3.6). Since each of these pairs anti-commutes, its commutator is twice its ordered product. Hence the commutator is the sum of the local obstructions

$$2 \left(A_j \tilde{B}_{j+1} + B_j \tilde{A}_j \right) \quad (3.17)$$

and

$$2 \left(A_{j+1} \tilde{B}_j + B_{j+2} \tilde{A}_j \right), \quad (3.18)$$

with boundary terms included only when the indices exist. Expanding the cubic definitions gives

$$2 \left(A_j \tilde{B}_{j+1} + B_j \tilde{A}_j \right) = 2i \left(\lambda_j - \tilde{\lambda}_j \right) B_j B_{j+1} \tilde{B}_j \tilde{B}_{j+1}, \quad (3.19)$$

$$2 \left(A_{j+1} \tilde{B}_j + B_{j+2} \tilde{A}_j \right) = 2i \left(\tilde{\lambda}_j - \lambda_{j+1} \right) B_{j+1} B_{j+2} \tilde{B}_j \tilde{B}_{j+1}. \quad (3.20)$$

Therefore (3.15) and (3.16) are sufficient for commutativity. In the abstract algebra the normal monomials in (3.19) and (3.20) are independent, so their coefficients must vanish. This gives $\lambda_j = \tilde{\lambda}_j$ and $\lambda_{j+1} = \tilde{\lambda}_j$ and proves necessity. \square

4 Independent free-fermion structure

We now investigate the two Hamiltonians separately and show that they are integrable and free-fermionic.

We will use the techniques of [7, 8]. In this section we will proceed as if the terms of H_1 and H_2 were algebraically independent, and then we can use the calculations of [7, 8] directly. The key point is that we focus on either H_1 or H_2 , but here we will not yet treat their linear combinations. This implies that we can choose either the set $\{\{B_j\}_{j=1,\dots,M}, \{A_k\}_{k=1,\dots,M-1}\}$ or $\{\{\tilde{B}_j\}_{j=1,\dots,M}, \{\tilde{A}_k\}_{k=1,\dots,M-1}\}$ as independent generators.

This procedure is justified as long as we do not consider H_1 and H_2 at the same time (we do not diagonalize their linear combinations).

4.1 Free fermions behind the disguise

We now recall the key results of [7, 8]. The reader who is familiar with this construction may skip this subsection.

Let

$$H = \sum_{v \in V} g_v \quad (4.1)$$

be a Hamiltonian whose terms are Hermitian graph-Clifford generators [11],

$$g_v = g_v^\dagger, \quad g_v^2 = w_v^2 \mathbf{1}, \quad (4.2)$$

and assume that each pair of distinct generators either commutes or anti-commutes. The frustration graph $G = G(H)$ has vertex set V , with an edge between v and v' precisely when

$$\{g_v, g_{v'}\} = 0. \quad (4.3)$$

Thus non-adjacent vertices correspond to commuting generators.

A hole is an induced cycle of length at least four, and an even hole is a hole with an even number of vertices. A claw is an induced copy of the graph $K_{1,3}$ (see Fig. 3). We say that G is ECF if it is

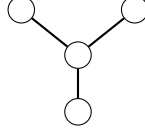


Figure 3: The claw graph

both even-hole-free and claw-free. We shall also use a simplicial clique $K \subset V$: this is a non-empty clique such that, for every $v \in K$, the set $N_G(v) \setminus K$ induces a clique. For ECF graphs such a simplicial clique exists, and it gives an edge operator χ satisfying

$$\chi = \chi^\dagger, \quad \chi^2 = \mathbf{1}, \quad \{\chi, g_v\} = 0 \quad (v \in K), \quad [\chi, g_v] = 0 \quad (v \notin K). \quad (4.4)$$

The operator χ may be adjoined algebraically if it is not already present in the representation.

Let $\mathcal{I}(G)$ be the set of independent sets of G , and let $\mathcal{I}_r(G) \subset \mathcal{I}(G)$ denote the independent sets of size r . We write

$$\mathcal{S}(G) = \max_{S \in \mathcal{I}(G)} |S|$$

for the independence number. For $S \in \mathcal{I}(G)$ define

$$g_S = \prod_{v \in S} g_v, \quad g_\emptyset = \mathbf{1}. \quad (4.5)$$

The order in this product is immaterial, because all generators belonging to an independent set commute. The independent-set charges are

$$Q_G^{(r)} = \sum_{S \in \mathcal{I}_r(G)} g_S, \quad r = 0, \dots, \mathcal{S}(G), \quad (4.6)$$

with $Q_G^{(0)} = \mathbf{1}$ and $Q_G^{(1)} = H$. If G is claw-free, then

$$[Q_G^{(r)}, Q_G^{(s)}] = 0 \quad (r, s = 0, \dots, \mathcal{S}(G)). \quad (4.7)$$

Equivalently, the transfer matrix

$$T_G(u) = \sum_{r=0}^{\mathcal{S}(G)} (-u)^r Q_G^{(r)} = \sum_{S \in \mathcal{I}(G)} (-u)^{|S|} g_S \quad (4.8)$$

forms a commuting family,

$$[T_G(u), T_G(v)] = 0. \quad (4.9)$$

It is normalized by

$$T_G(0) = \mathbf{1}, \quad -\partial_u T_G(0) = H. \quad (4.10)$$

The weighted independence polynomial is

$$P_G(x) = \sum_{S \in \mathcal{I}(G)} (-x)^{|S|} \prod_{v \in S} w_v^2. \quad (4.11)$$

If G is ECF, the transfer matrix obeys the inversion relation

$$T_G(u)T_G(-u) = P_G(u^2)\mathbf{1}. \quad (4.12)$$

For generic non-zero weights we write

$$P_G(x) = \prod_{k=1}^{\mathcal{S}(G)} (1 - \varepsilon_k^2 x), \quad u_k = \varepsilon_k^{-1}. \quad (4.13)$$

The numbers ε_k are the one-particle energies.

The hidden fermionic operators are obtained by dressing the edge operator with the transfer matrix:

$$\Psi_k = C_k T_G(-u_k) \chi T_G(u_k), \quad \Psi_{-k} = C_k T_G(u_k) \chi T_G(-u_k), \quad k = 1, \dots, \mathcal{S}(G). \quad (4.14)$$

The constants C_k are chosen so that the canonical anti-commutation relations hold,

$$\{\Psi_k, \Psi_\ell\} = \delta_{k+\ell} \mathbf{1}. \quad (4.15)$$

The normalization factor is

$$C_k^{-2} = -16u_k^2 P_{G \setminus K}(u_k^2) P'_G(u_k^2), \quad (4.16)$$

where $P_{G \setminus K}$ is the polynomial (4.11) for the induced graph obtained by deleting the simplicial clique K .

The operators $\Psi_{\pm k}$ are ladder operators for H :

$$[H, \Psi_{\pm k}] = \pm 2\varepsilon_k \Psi_{\pm k}. \quad (4.17)$$

Moreover, the Hamiltonian itself is reconstructed as the free-fermion quadratic form

$$H = \sum_{k=1}^{\mathcal{S}(G)} \varepsilon_k [\Psi_k, \Psi_{-k}]. \quad (4.18)$$

Thus

$$\text{Spec}(H) = \left\{ \sum_{k=1}^{\mathcal{S}(G)} s_k \varepsilon_k : s_k = \pm 1 \right\}, \quad (4.19)$$

up to the homogeneous degeneracy coming from degrees of freedom not resolved by these $\mathcal{S}(G)$ hidden fermions.

4.2 The origin of exponential degeneracies

Here we explain why it is difficult to find FFD-type models that are free from exponential degeneracies, based on the results quoted in the last subsection. The key observation is that in such models the number of fermionic eigenmodes is given by \mathcal{S} , the independence number of the frustration graph, which is typically smaller than the number of qubits needed for the representations of the algebras.

If a graph-Clifford algebra has M generators, and it describes a lattice spin model, then $\mathcal{S} \sim M$. In a connected claw-free graph the maximal possible asymptotic \mathcal{S}/M ratio is $1/2$. This is a classic result in graph theory [17, 18]: the maximum value of \mathcal{S} for a connected claw-free graph is $\lceil M/2 \rceil$. It follows that the maximal number of fermionic eigenmodes is $\lceil M/2 \rceil$. In the models that appeared in the literature the bound was reached only by the Ising/ XY families, whose frustration graphs are the path or circle graphs, for open or periodic boundary conditions, respectively. In other FFD-type

models that have appeared in the literature, the asymptotic \mathcal{S}/M ratio was smaller; in the case of the FFD model, this ratio is $1/3$.

If a graph-Clifford algebra is non-degenerate (has a trivial center), or the dimension of the center is bounded, then the algebra can be represented on $N = M/2 + \mathcal{O}(1)$ qubits [11]. There are no smaller representations.

This implies that in every case in which the asymptotic \mathcal{S}/M ratio is smaller than $1/2$, there will be exponential degeneracies due to the missing number of eigenmodes. In the case of the FFD model the degeneracies were recently tied to new families of hidden fermions [10].

These arguments show that for many graph-Clifford algebras which are more complicated than the Ising-type algebras one would need an extensive number of independent central elements, so that the dimension of the representations can be lowered. In parallel, one might need to work with generalizations of the framework of [7, 8], in order to avoid the strong requirements for the ECF graphs.

We will see that our model uses both mechanisms together to avoid the appearance of the exponential degeneracies. We will return to this issue in the Conclusions, see Section 8.

Finally, we also remark that the upper bound for the independence number is reached in many other connected claw-free graphs or graph families. However, the corresponding models might not have an interpretation as a spin-chain model, or they might be related to Jordan-Wigner solvable models by simple unitary transformations. This open direction is left for further research.

4.3 Frustration graphs and simplicial cliques in our model

We now apply the formalism presented above to H_1 and H_2 .

Let Γ_1 be the graph whose vertices are the generators of H_1 , with an edge between two vertices exactly when the corresponding algebra elements anti-commute. Lemma 3.1 identifies Γ_1 with a particular interval graph. The frustration graph for H_2 is identical.

Interval graphs are chordal, hence contain no induced cycle of length at least four. In the present interval family they are also claw-free: one interval of length two or three cannot meet three pairwise disjoint intervals of length at least two. Therefore Γ_1 is ECF.

We now discuss the issue of the algebraic relations between the various terms of the two Hamiltonians. Our main claim is that we can immediately apply the results of [7, 8] if we treat H_1 and H_2 independently. The reason for this is that although the operators A_j are products in the larger algebra, the family $\{B_j, A_j\}$ has no further algebraic relations. This is shown as follows. After rescaling the generators to involutions, a monomial $\prod_j B_j^{x_j} \prod_j A_j^{y_j}$, with $x_j, y_j \in \{0, 1\}$, has tilded exponents y_j in the normal form of the two Ising algebras. Hence a scalar monomial must have all $y_j = 0$, and then the untilded exponents force all $x_j = 0$. Thus the subalgebra generated by $\{B_j, A_j\}$ is the graph-Clifford algebra with frustration graph Γ_1 . The tilded family is analogous.

These arguments imply that the Hamiltonians H_1 and H_2 separately possess an extensive number of conserved quantities, and they can be solved by free-fermionic operators.

The construction of [7, 8] uses a so-called edge operator, which is associated with a simplicial clique in the graph. The left boundary pair

$$K_1 = \{A_1, B_1\} \tag{4.20}$$

is a simplicial clique for Γ_1 . This means that we need to find an operator $\chi_1 = \chi_1^\dagger$ with $\chi_1^2 = \mathbf{1}$ such that

$$\{\chi_1, A_1\} = \{\chi_1, B_1\} = 0, \quad [\chi_1, g] = 0 \quad \text{for all other generators } g \text{ of } H_1. \tag{4.21}$$

In the abstract treatment such an operator can be chosen as an additional generator, and in some cases it can be chosen to lie within the algebra itself [11]. We do not discuss these subtleties at this

point; instead we state only that a suitable χ_1 can be found in our concrete representations. This is enough to construct the free-fermionic operators that solve the Hamiltonians.

For H_2 it is natural to choose the simplicial clique to lie at the other boundary:

$$K_2 = \{\tilde{A}_{M-1}, \tilde{B}_M\}. \quad (4.22)$$

In this way, we can construct mutually commuting or anti-commuting ladder operators for the two Hamiltonians, see Section 5. If we chose K_1 as the simplicial clique for H_2 , then we would not be able to construct cross-compatible operators for $\lambda \neq 0$, see the remark at the end of Section 5.

4.4 Transfer matrices

We now derive transfer matrices using the methods of [7, 8]. We will denote by $0 < m \leq M$ the subalgebras corresponding to smaller spin chains, and we will derive recursions in m . The full chain corresponds to $m = M$.

Consider m short generators, and let \mathcal{I}_m be the set of independent sets in the interval family

$$\{I(B_j)\}_{j=1}^m \cup \{I(A_j)\}_{j=1}^{m-1}.$$

For $m = 0, 1$ the second set is empty. For $S \in \mathcal{I}_m$, let $g_1(S)$ be the product of the corresponding H_1 generators, ordered by increasing left endpoint. Let $g_2(S)$ be the same ordered product with all generators tilded. The order is immaterial inside an independent set, because its generators commute.

Definition 4.1. For $0 \leq m \leq M$, define the prefix transfer matrices by

$$T_{1,m}(u) = \sum_{S \in \mathcal{I}_m} (-u)^{|S|} g_1(S), \quad T_{2,m}(u) = \sum_{S \in \mathcal{I}_m} (-u)^{|S|} g_2(S). \quad (4.23)$$

The full transfer matrices are the $m = M$ members. They are normalized by

$$-\partial_u T_{1,M}(0) = H_1, \quad -\partial_u T_{2,M}(0) = H_2. \quad (4.24)$$

Remark 4.2. The order of the transfer matrices in u is determined by the independence number of the frustration graph, $\mathcal{S} = \lfloor \frac{M+1}{2} \rfloor$.

Proposition 4.3 (Boundary recursion). For $m \geq 3$,

$$T_{1,m}(u) = T_{1,m-1}(u) - uB_m T_{1,m-2}(u) - uA_{m-1} T_{1,m-3}(u), \quad (4.25)$$

$$T_{2,m}(u) = T_{2,m-1}(u) - u\tilde{B}_m T_{2,m-2}(u) - u\tilde{A}_{m-1} T_{2,m-3}(u), \quad (4.26)$$

with initial conditions

$$T_{a,0}(u) = 1, \quad T_{1,1}(u) = 1 - uB_1, \quad T_{2,1}(u) = 1 - u\tilde{B}_1, \quad (4.27)$$

and

$$T_{1,2}(u) = 1 - u(B_1 + B_2 + A_1), \quad T_{2,2}(u) = 1 - u(\tilde{B}_1 + \tilde{B}_2 + \tilde{A}_1). \quad (4.28)$$

Proof. An independent set in \mathcal{I}_m is exactly one of the following: it uses no generator touching the right endpoint of the chain, giving an independent set in \mathcal{I}_{m-1} ; it uses the short generator B_m (or \tilde{B}_m), in which case the rest lies in \mathcal{I}_{m-2} ; or it uses the long generator A_{m-1} (or \tilde{A}_{m-1}), in which case the rest lies in \mathcal{I}_{m-3} . This is precisely (4.25) and (4.26). The displayed initial conditions are the direct independent-set sums for zero, one, and two short generators. \square

4.5 Inversion relation and one-particle energies

For each family, the inversion relation is a purely algebraic cancellation among independent-set monomials.

Theorem 4.4 (Independent inversion relation). *For $a = 1, 2$,*

$$T_{a,M}(u)T_{a,M}(-u) = P_{a,M}(u^2)\mathbf{1}, \quad (4.29)$$

where $P_{a,M}$ is the weighted independence polynomial of order \mathcal{S} , given by

$$P_{a,M}(x) = \sum_{S \in \mathcal{I}_M} (-x)^{|S|} \prod_{g \in S} w_a(g)^2. \quad (4.30)$$

Here $w_a(g)^2$ denotes the scalar square of the generator g in the a -th family. Thus

$$w_1(B_j)^2 = \beta_j^2, \quad w_1(A_j)^2 = \alpha_j^2, \quad (4.31)$$

$$w_2(\tilde{B}_j)^2 = \tilde{\beta}_j^2, \quad w_2(\tilde{A}_j)^2 = \tilde{\alpha}_j^2. \quad (4.32)$$

Proof. As long as we treat the two transfer matrices separately, the formalism of [7, 8] applies directly. The frustration graphs of H_1 and H_2 are identical and this graph is ECF. The statement of the theorem follows immediately. \square

Proposition 4.5 (Inhomogeneous recursion for $P_{a,m}$). *For the polynomials defined by (4.30) with M replaced by m , set*

$$P_{a,0}(x) = 1.$$

Then

$$P_{1,1}(x) = 1 - x\beta_1^2, \quad P_{2,1}(x) = 1 - x\tilde{\beta}_1^2,$$

and

$$P_{1,2}(x) = 1 - x(\beta_1^2 + \beta_2^2 + \alpha_1^2), \quad P_{2,2}(x) = 1 - x(\tilde{\beta}_1^2 + \tilde{\beta}_2^2 + \tilde{\alpha}_1^2).$$

For $m \geq 3$ one has

$$P_{1,m}(x) = P_{1,m-1}(x) - x\beta_m^2 P_{1,m-2}(x) - x\alpha_{m-1}^2 P_{1,m-3}(x), \quad (4.33)$$

$$P_{2,m}(x) = P_{2,m-1}(x) - x\tilde{\beta}_m^2 P_{2,m-2}(x) - x\tilde{\alpha}_{m-1}^2 P_{2,m-3}(x). \quad (4.34)$$

Proof. Decompose an independent set according to the right boundary. It either contains no generator touching the right endpoint, giving $P_{a,m-1}$; or it contains the short interval B_m or \tilde{B}_m , leaving an independent set in \mathcal{I}_{m-2} ; or it contains the long interval A_{m-1} or \tilde{A}_{m-1} , leaving an independent set in \mathcal{I}_{m-3} . Multiplying by the corresponding scalar squares gives the stated recursion. \square

Consider the factorization

$$P_{a,M}(x) = \prod_{k=1}^{\mathcal{S}} (1 - \varepsilon_{a,k}^2 x). \quad (4.35)$$

We can now state the main result of this section: using the constructions of [7, 8] we obtain free-fermionic operators $\Psi_{a,k}$ such that

$$H_a = \sum_k \varepsilon_{a,k} \mathcal{Z}_{a,k}, \quad \mathcal{Z}_{a,k} \equiv [\Psi_{a,k}, \Psi_{a,-k}]. \quad (4.36)$$

The corresponding Dirac operators are obtained from an edge operator by the standard transfer-matrix formula

$$\Psi_{a,\pm k} = C_{a,k} T_{a,M}(\mp u_{a,k}) \chi_a T_{a,M}(\pm u_{a,k}), \quad u_{a,k} = \varepsilon_{a,k}^{-1}, \quad (4.37)$$

where $C_{a,k}$ is the normalization factor obtained from the general formula (4.16).

5 Mutual free-fermion structure

We now establish the compatibility of the fermionic structures constructed earlier separately for H_1 and H_2 . From now on, we work in the global- λ family (2.11), so that $[H_1, H_2] = 0$.

First we prove the commutativity of the mode occupation operators $\mathcal{Z}_{a,k}$ introduced in (4.36).

Then we prove the cross-commutativity of the transfer matrices and show that we can choose appropriate edge operators such that the fermionic ladder operators themselves are compatible.

5.1 Cross-commutativity of the mode occupation operators

Proposition 5.1 (Mode occupations as polynomials in one Hamiltonian). *Fix $a \in \{1, 2\}$. Assume that the same-family hidden fermions have already been constructed, so that*

$$H_a = \sum_{r=1}^S \varepsilon_{a,r} \mathcal{Z}_{a,r}, \quad \mathcal{Z}_{a,r} = [\Psi_{a,r}, \Psi_{a,-r}], \quad (5.1)$$

with

$$\mathcal{Z}_{a,r}^2 = \mathbf{1}, \quad [\mathcal{Z}_{a,r}, \mathcal{Z}_{a,s}] = 0. \quad (5.2)$$

Assume also the generic non-resonance condition

$$E_a(\sigma) \neq E_a(\tau) \quad \text{for all } \sigma \neq \tau, \quad \sigma, \tau \in \{\pm 1\}^S, \quad (5.3)$$

where

$$E_a(\sigma) = \sum_{r=1}^S \sigma_r \varepsilon_{a,r}. \quad (5.4)$$

Then each mode occupation involution $\mathcal{Z}_{a,k}$ is a polynomial in H_a . More precisely,

$$\mathcal{Z}_{a,k} = z_{a,k}(H_a), \quad (5.5)$$

where the interpolation polynomial is

$$z_{a,k}(x) = \sum_{\sigma \in \{\pm 1\}^S} \sigma_k \prod_{\substack{\tau \in \{\pm 1\}^S \\ \tau \neq \sigma}} \frac{x - E_a(\tau)}{E_a(\sigma) - E_a(\tau)}. \quad (5.6)$$

Proof. We first construct the projectors that select the different sign patterns. Since the operators $\mathcal{Z}_{a,r}$ are commuting involutions, the operators

$$\Pi_a(\sigma) = 2^{-S} \prod_{r=1}^S (\mathbf{1} + \sigma_r \mathcal{Z}_{a,r}), \quad \sigma \in \{\pm 1\}^S, \quad (5.7)$$

are mutually orthogonal idempotents and satisfy

$$\sum_{\sigma \in \{\pm 1\}^S} \Pi_a(\sigma) = \mathbf{1}. \quad (5.8)$$

Moreover,

$$\mathcal{Z}_{a,k} \Pi_a(\sigma) = \sigma_k \Pi_a(\sigma). \quad (5.9)$$

Therefore, using (5.1) we obtain

$$H_a \Pi_a(\sigma) = \left(\sum_{r=1}^{\mathcal{S}} \sigma_r \varepsilon_{a,r} \right) \Pi_a(\sigma) = E_a(\sigma) \Pi_a(\sigma).$$

Consequently

$$H_a = \sum_{\sigma \in \{\pm 1\}^{\mathcal{S}}} E_a(\sigma) \Pi_a(\sigma). \quad (5.10)$$

More generally, for every polynomial f ,

$$f(H_a) = \sum_{\sigma \in \{\pm 1\}^{\mathcal{S}}} f(E_a(\sigma)) \Pi_a(\sigma). \quad (5.11)$$

Indeed, this follows from $H_a^m \Pi_a(\sigma) = E_a(\sigma)^m \Pi_a(\sigma)$ and linearity.

By the non-resonance assumption (5.3), the numbers $E_a(\sigma)$ are pairwise distinct. Hence the Lagrange polynomial (5.6) is well-defined and satisfies

$$z_{a,k}(E_a(\sigma)) = \sigma_k \quad \text{for all } \sigma \in \{\pm 1\}^{\mathcal{S}}. \quad (5.12)$$

Therefore

$$z_{a,k}(H_a) = \sum_{\sigma \in \{\pm 1\}^{\mathcal{S}}} z_{a,k}(E_a(\sigma)) \Pi_a(\sigma) = \sum_{\sigma \in \{\pm 1\}^{\mathcal{S}}} \sigma_k \Pi_a(\sigma) = \mathcal{Z}_{a,k}. \quad (5.13)$$

This proves (5.5). \square

Corollary 5.2 (Cross-commutativity of the mode occupations). *In the global- λ family, and on the common non-resonant locus (5.3) for $a = 1, 2$, the mode occupation operators of the two hidden free-fermion structures commute:*

$$[\mathcal{Z}_{1,i}, \mathcal{Z}_{2,j}] = 0, \quad i, j = 1, \dots, \mathcal{S}. \quad (5.14)$$

Proof. By Theorem 3.3, in the global- λ family we have

$$[H_1, H_2] = 0. \quad (5.15)$$

Using Proposition 5.1, we may write

$$\mathcal{Z}_{1,i} = z_{1,i}(H_1), \quad \mathcal{Z}_{2,j} = z_{2,j}(H_2). \quad (5.16)$$

But polynomials in commuting operators commute. Hence

$$[\mathcal{Z}_{1,i}, \mathcal{Z}_{2,j}] = [z_{1,i}(H_1), z_{2,j}(H_2)] = 0. \quad (5.17)$$

\square

Corollary 5.3 (Free fermions in the linear combinations). *The linear combinations $H_1 \pm H_2$ are free-fermionic, and their spectrum is given by*

$$E(\sigma, \tau) = \sum_{r=1}^{\mathcal{S}} \sigma_r \varepsilon_{1,r} \pm \sum_{r=1}^{\mathcal{S}} \tau_r \varepsilon_{2,r}, \quad \sigma_r, \tau_r \in \{\pm 1\}, \quad \mathcal{S} = \left\lfloor \frac{M+1}{2} \right\rfloor, \quad (5.18)$$

where the single-particle energies $\varepsilon_{a,r}$ with $a = 1, 2$ are computed from the roots of the polynomials $P_{a,M}(x)$.

At this stage we can conveniently prove the following:

Theorem 5.4 (Cross-commutativity of the transfer matrices). *For all spectral parameters u, v ,*

$$[T_{1,M}(u), T_{2,M}(v)] = 0. \quad (5.19)$$

Consequently all higher charges generated by the two transfer matrices commute across the two families.

Proof. The single-family free-fermion diagonalization gives [7, 8]

$$T_{a,M}(u) = \prod_{k=1}^S (1 - u\varepsilon_{a,k} \mathcal{Z}_{a,k}), \quad \mathcal{Z}_{a,k} = [\Psi_{a,k}, \Psi_{a,-k}].$$

The occupation involutions commute within each family. Their cross-commutativity was proved in Corollary 5.2. Therefore every factor in $T_{1,M}(u)$ commutes with every factor in $T_{2,M}(v)$, proving the theorem. \square

5.2 Compatible edge operators and Dirac fermions

To have compatible fermionic operators, the edge operators must also be compatible with the opposite transfer matrix. Algebraically, we require

$$[\chi_1, \tilde{A}_j] = [\chi_1, \tilde{B}_j] = 0, \quad [\chi_2, A_j] = [\chi_2, B_j] = 0 \quad \text{for all } j. \quad (5.20)$$

Then

$$[\chi_1, T_{2,m}(v)] = 0, \quad [\chi_2, T_{1,m}(u)] = 0 \quad (5.21)$$

for every $0 \leq m \leq M$ and all u, v .

The two simplicial cliques we chose earlier are

$$K_1 = \{A_1, B_1\}, \quad K_2 = \{\tilde{A}_{M-1}, \tilde{B}_M\}. \quad (5.22)$$

Recall that

$$A_j = i\lambda_j B_j B_{j+1} \tilde{B}_j, \quad \tilde{A}_j = -i\tilde{\lambda}_j \tilde{B}_j \tilde{B}_{j+1} B_{j+1}, \quad (j = 1, \dots, M-1). \quad (5.23)$$

This means that if

$$\begin{aligned} \{\chi_1, B_1\} &= 0, & [\chi_1, B_j] &= 0 \quad j > 1, \\ \{\chi_2, \tilde{B}_M\} &= 0, & [\chi_2, \tilde{B}_j] &= 0 \quad j < M, \end{aligned} \quad (5.24)$$

and if the A_j and \tilde{A}_j are given by the cubic products above while the cross-commutation relations (5.20) are also satisfied, then the edge operators are compatible with the simplicial cliques chosen above.

There are two useful choices for the mutual relation of the two edge operators:

$$[\chi_1, \chi_2] = 0 \quad (5.25)$$

or

$$\{\chi_1, \chi_2\} = 0. \quad (5.26)$$

In these cases we obtain simple cross-relations between the fermionic operators. Indeed, we can show using (4.37), Theorem 5.4, and the edge-transfer relations above, that the commutation relations of the two hidden Dirac families are given by

$$\Psi_{1,k}\Psi_{2,\ell} = \eta \Psi_{2,\ell}\Psi_{1,k}, \quad \eta = \begin{cases} +1, & [\chi_1, \chi_2] = 0, \\ -1, & \{\chi_1, \chi_2\} = 0. \end{cases} \quad (5.27)$$

We now consider the Ising and XY representations and find concrete edge operators satisfying all the necessary conditions. For simplicity we focus on the case of (5.25), which leads to commuting families of fermionic ladder operators. In this case the edge operators can be chosen as completely localized operators in both representations. It is also possible to find appropriate $\chi_{1,2}$ in the anti-commuting case, but then one of them needs to be a non-local operator product.

In the Ising case we denote by $n = \lceil (M+1)/2 \rceil$ the number of spins on one chain. For the edge operators we can choose for example

$$\chi_1 = \sigma_1^x, \quad \chi_2 = \begin{cases} \tau_n^x & M \text{ odd} \\ \tau_n^z & M \text{ even} \end{cases}. \quad (5.28)$$

In the XY case we can choose

$$\chi_1 = X_1, \quad \chi_2 = X_{M+1}. \quad (5.29)$$

These choices satisfy all requirements.

Finally, we remark that if we had chosen K_1 as the simplicial clique for both H_1 and H_2 , then we would not be able to satisfy all the necessary conditions for the edge operators, irrespective of the representation. A putative edge operator χ_2 would need to obey

$$\{\chi_2, \tilde{B}_1\} = 0, \quad \{\chi_2, \tilde{A}_1\} = 0,$$

and cross-compatibility with H_1 would require

$$[\chi_2, B_j] = [\chi_2, A_j] = 0 \quad \text{for all } j.$$

However,

$$A_1 = i\lambda_1 B_1 B_2 \tilde{B}_1.$$

Thus $[\chi_2, B_1] = [\chi_2, B_2] = 0$, together with $\{\chi_2, \tilde{B}_1\} = 0$, forces

$$\{\chi_2, A_1\} = 0,$$

contradicting the required condition $[\chi_2, A_1] = 0$. Therefore the same-left-boundary choice cannot give cross-compatible edge operators.

6 The degeneracies in the spectrum

We are now in a position to discuss our main claims about the spectrum and its degeneracies. It follows from the previous sections that the energy eigenvalues are of the form (5.18). We now discuss the degeneracies of these energy values, both in the Ising and XY representations.

Assume that the coupling constants $\beta_j, \tilde{\beta}_j, j = 1, \dots, M$ are generic numbers, and in particular, the two sets are not related to each other in any way. Fix a finite M and tune the perturbation

strength λ continuously from 0 to some finite value. Switching on an infinitesimal λ can split existing degeneracies, but it cannot increase them, except at isolated points in parameter space. At the same time, the energy formula above is rigid; in particular, the number of fermionic eigenmodes \mathcal{S} is the same for $\lambda = 0$ and for a non-zero λ . Only the one-particle energies change as a function of λ . It follows that the degeneracies are exactly the same for $\lambda = 0$ and a finite non-zero λ , at least in a small neighbourhood of $\lambda = 0$.

The actual degeneracies can be computed using simple counting arguments:

- For $M = 2\ell + 1$ the number of qubits used in the two representations is the same, given by $N = 2\ell + 2$. The number of fermionic eigenmodes is $\mathcal{S} = \ell + 1$ for each Hamiltonian H_1 and H_2 ; therefore the total number of eigenmodes coincides with the number of qubits. This implies that every energy level is non-degenerate.
- For $M = 2\ell$ the number of qubits used in the two representations is not the same: we have $N = 2\ell + 2$ and $N = 2\ell + 1$ qubits in the Ising and XY representations, respectively. The total number of eigenmodes is $2\mathcal{S} = 2\ell$. This implies that every energy level is degenerate with a homogeneous degeneracy of 4 and 2 in the Ising and XY representations, respectively.

In Appendix A we present concrete numerical evidence for the free-fermionic spectrum and these degeneracies, in the case of the XY representation.

If we impose more symmetry on the combinations $H_1 \pm H_2$, then the degeneracy pattern can change substantially. For example, in the homogeneous case $\beta_j = \tilde{\beta}_j = \beta$, the two Hamiltonians have identical single-particle energies. As a result, the degeneracies of the energy eigenvalues will not be homogeneous. In particular, the null spaces of $H_1 \pm H_2$ will be exponentially degenerate.

7 The homogeneous chain

Here we treat the homogeneous chain and derive the dispersion relations and the standing-wave equations for the quasi-momenta of the fermionic excitations. We show that these quantities also interpolate between the corresponding quantities of the XY and FFD models.

We use the normalization

$$\beta_j = \tilde{\beta}_j = 1 \quad (j = 1, \dots, M), \quad \lambda_j = \tilde{\lambda}_j = \lambda \quad (j = 1, \dots, M - 1). \quad (7.1)$$

Thus, for both families,

$$B_j^2 = \tilde{B}_j^2 = \mathbf{1}, \quad A_j^2 = \tilde{A}_j^2 = \lambda^2 \mathbf{1}. \quad (7.2)$$

We assume $\lambda > 0$ in the dispersion formulas. The scalar spectral data only depend on λ^2 , so changing the sign of λ does not change the one-particle energies.

The two families have the same weighted independence polynomial, and the single-particle energies will be identical.

For either family let $N_A(S)$ be the number of long generators in the independent set S ; that is, the number of A_j 's in the untilded family or \tilde{A}_j 's in the tilded family. Then

$$P_M^{(\lambda)}(x) = \sum_{S \in \mathcal{I}_M} (-x)^{|S|} \lambda^{2N_A(S)}. \quad (7.3)$$

If

$$P_M^{(\lambda)}(x) = \prod_{k=1}^{\mathcal{S}} (1 - \varepsilon_k(\lambda)^2 x), \quad \mathcal{S} = \left\lfloor \frac{M+1}{2} \right\rfloor, \quad (7.4)$$

then $x_k = \varepsilon_k(\lambda)^{-2}$ are the roots of $P_M^{(\lambda)}$. In the present symmetric homogeneous case these are the one-particle energies for both H_1 and H_2 :

$$\varepsilon_{1,k} = \varepsilon_{2,k} = \varepsilon_k(\lambda). \quad (7.5)$$

Consequently the scalar part of the spectrum of $H_1 \pm H_2$ is obtained from two identical copies of this set of one-particle energies, as in (5.18).

Corollary 7.1 (Polynomial recursion). *The homogeneous polynomial in the normalization (7.1) satisfies*

$$P_M^{(\lambda)}(x) = P_{M-1}^{(\lambda)}(x) - xP_{M-2}^{(\lambda)}(x) - \lambda^2 x P_{M-3}^{(\lambda)}(x), \quad (M \geq 3), \quad (7.6)$$

with

$$P_0^{(\lambda)}(x) = 1, \quad P_1^{(\lambda)}(x) = 1 - x, \quad P_2^{(\lambda)}(x) = 1 - (2 + \lambda^2)x. \quad (7.7)$$

The generating function is

$$\sum_{M \geq 0} P_M^{(\lambda)}(x) t^M = \frac{1 - xt - \lambda^2 x t^2}{1 - t + x t^2 + \lambda^2 x t^3}. \quad (7.8)$$

Proof. Decompose an independent set by the largest right endpoint. It either uses no generator touching the right boundary, uses the short generator B_M or \tilde{B}_M , or uses the long generator A_{M-1} or \tilde{A}_{M-1} . The short weight is 1 and the long weight is λ^2 , giving the three terms in (7.6). The initial values are the direct independent-set sums for algebra sizes 0, 1, 2. The generating function follows by summing the recursion with these initial values. \square

Equivalently,

$$P_M^{(\lambda)}(x) = \sum_{\substack{r,s \geq 0 \\ 2r+3s \leq M+1}} (-x)^{r+s} \lambda^{2s} \binom{M+1-r-2s}{r+s} \binom{r+s}{r}, \quad (7.9)$$

where r is the number of short generators and s is the number of long generators.

7.1 Bulk dispersion and finite-size standing waves

For fixed x , the characteristic equation of (7.6) is

$$\mu^3 - \mu^2 + x\mu + \lambda^2 x = 0. \quad (7.10)$$

For the physical branch with $x > 0$, write the complex conjugate pair and the real root as

$$\mu_{\pm} = B_{\lambda} e^{\pm i p}, \quad \mu_0 = 1 - U_{\lambda}, \quad U_{\lambda} = 2B_{\lambda} \cos p, \quad 0 < p < \frac{\pi}{2}. \quad (7.11)$$

Vieta's relations give

$$U_{\lambda}^2 + (4\lambda^2 \cos^2 p - 1 - \lambda^2)U_{\lambda} - 4\lambda^2 \cos^2 p = 0. \quad (7.12)$$

The physical solution is

$$U_{\lambda}(p) = \frac{1 + \lambda^2 - 4\lambda^2 \cos^2 p + \sqrt{(1 + \lambda^2 - 4\lambda^2 \cos^2 p)^2 + 16\lambda^2 \cos^2 p}}{2}. \quad (7.13)$$

Then

$$B_\lambda(p) = \frac{U_\lambda(p)}{2 \cos p}, \quad x_\lambda(p) = \frac{U_\lambda(p)^2 (U_\lambda(p) - 1)}{4\lambda^2 \cos^2 p}, \quad (7.14)$$

and the one-particle dispersion is

$$\varepsilon_\lambda(p) = \frac{1}{\sqrt{x_\lambda(p)}} = \frac{2\lambda \cos p}{U_\lambda(p) \sqrt{U_\lambda(p) - 1}}. \quad (7.15)$$

The exact finite-size formula follows from partial fractions. If the three roots of (7.10) are denoted by μ_+ , μ_- , and μ_0 , then

$$P_M^{(\lambda)}(x) = \sum_{a \in \{+, -, 0\}} \frac{\mu_a^{M+3}}{\prod_{b \neq a} (\mu_a - \mu_b)}. \quad (7.16)$$

The decomposition is valid if the roots are all distinct, which is justified for almost all values of p .

Define

$$z_\lambda(p) := \mu_+ - \mu_0 = B_\lambda(p) e^{ip} - (1 - U_\lambda(p)) = \rho_\lambda(p) e^{i\delta_\lambda(p)}. \quad (7.17)$$

Then

$$\rho_\lambda(p) = \sqrt{(3B_\lambda(p) \cos p - 1)^2 + B_\lambda(p)^2 \sin^2 p}, \quad \delta_\lambda(p) = \arctan \frac{U_\lambda(p) \tan p}{3U_\lambda(p) - 2}. \quad (7.18)$$

A direct simplification gives

$$P_M^{(\lambda)}(x_\lambda(p)) = \frac{B_\lambda(p)^{M+2}}{\rho_\lambda(p) \sin p} \sin((M+3)p - \delta_\lambda(p)) + \frac{(1 - U_\lambda(p))^{M+3}}{\rho_\lambda(p)^2}. \quad (7.19)$$

Thus the exact root condition is

$$\sin((M+3)p_k - \delta_\lambda(p_k)) = -\frac{(1 - U_\lambda(p_k))^{M+3} \sin p_k}{\rho_\lambda(p_k) B_\lambda(p_k)^{M+2}}. \quad (7.20)$$

Since $|1 - U_\lambda(p)| < B_\lambda(p)$ on the physical branch, the right-hand side is exponentially small in M . The large- M standing-wave condition is

$$(M+3)p_k - \delta_\lambda(p_k) = \pi k + O\left(\left|\frac{1 - U_\lambda(p_k)}{B_\lambda(p_k)}\right|^{M+2}\right), \quad k = 1, \dots, \mathcal{S}. \quad (7.21)$$

7.2 Spectral edge

At fixed finite $\lambda > 0$ and $p \rightarrow \pi/2$,

$$\varepsilon_\lambda(p) \sim \frac{2}{1 + \lambda^2} \left(\frac{\pi}{2} - p\right), \quad (7.22)$$

so the smallest mode scales as M^{-1} .

7.3 The $\lambda \rightarrow 0$ limit

The endpoint $\lambda = 0$ is obtained as a regular degeneration of the finite- λ formulas. First, taking the limit in the closed form (7.9) suppresses all terms containing long generators:

$$P_M^{(0)}(x) := \lim_{\lambda \rightarrow 0} P_M^{(\lambda)}(x) = \sum_{\substack{r \geq 0 \\ 2r \leq M+1}} (-x)^r \binom{M+1-r}{r}. \quad (7.23)$$

Equivalently, the same limit in the recursion and the generating function gives

$$P_M^{(0)}(x) = P_{M-1}^{(0)}(x) - xP_{M-2}^{(0)}(x), \quad (M \geq 2), \quad P_0^{(0)} = 1, \quad P_1^{(0)} = 1 - x, \quad (7.24)$$

and

$$\sum_{M \geq 0} P_M^{(0)}(x)t^M = \frac{1 - xt}{1 - t + xt^2}. \quad (7.25)$$

We now take the limit directly in the finite- λ dispersion formulas. For fixed $0 < p < \pi/2$, write $c = \cos p$. From (7.13) one obtains

$$U_\lambda(p) = 1 + \lambda^2 - 4\lambda^4 c^2 + O(\lambda^6). \quad (7.26)$$

Substitution into (7.14) gives

$$x_\lambda(p) = \frac{1}{4c^2} [1 + 2(1 - 2c^2)\lambda^2 + O(\lambda^4)], \quad \varepsilon_\lambda(p) = 2c [1 + (2c^2 - 1)\lambda^2 + O(\lambda^4)]. \quad (7.27)$$

Thus the limiting parametrization is

$$x_0(p) = \frac{1}{4 \cos^2 p}, \quad \varepsilon_0(p) = 2 \cos p. \quad (7.28)$$

The finite-size standing-wave condition also has a direct limit. From (7.18),

$$B_\lambda(p) \longrightarrow \frac{1}{2 \cos p}, \quad \rho_\lambda(p) \longrightarrow \frac{1}{2 \cos p}, \quad \delta_\lambda(p) \longrightarrow p. \quad (7.29)$$

Moreover,

$$1 - U_\lambda(p) = -\lambda^2 + O(\lambda^4), \quad (7.30)$$

so the second term in (7.19) vanishes as $\lambda \rightarrow 0$. Taking the limit of (7.19) therefore gives

$$P_M^{(0)}(x_0(p)) = \frac{\sin((M+2)p)}{(2 \cos p)^{M+1} \sin p}. \quad (7.31)$$

The exact root condition follows immediately:

$$\sin((M+2)p_k) = 0. \quad (7.32)$$

Hence

$$(M+2)p_k = \pi k, \quad \varepsilon_k(0) = 2 \cos \frac{\pi k}{M+2}, \quad k = 1, \dots, \mathcal{S}. \quad (7.33)$$

This is the open-path one-particle quantization obtained as the $\lambda \rightarrow 0$ limit of the general standing-wave equation.

The same limiting calculation also gives the first correction to the momenta. For fixed M , the right-hand side of (7.20) is $O(\lambda^{2M+6})$, while

$$\delta_\lambda(p) = p - \lambda^2 \sin(2p) + O(\lambda^4). \quad (7.34)$$

Thus

$$(M+2)p_k + \lambda^2 \sin(2p_k) = \pi k + O(\lambda^4), \quad (7.35)$$

or, with $p_k^{(0)} = \pi k / (M+2)$,

$$p_k(\lambda) = p_k^{(0)} - \frac{\lambda^2}{M+2} \sin(2p_k^{(0)}) + O(\lambda^4). \quad (7.36)$$

7.4 The $\lambda \rightarrow \infty$ limit

The FFD endpoint is obtained from the finite- λ formulas after the natural rescaling

$$x = \frac{y}{\lambda^2}, \quad \widehat{\varepsilon} = \frac{\varepsilon}{\lambda}, \quad y = \frac{1}{\widehat{\varepsilon}^2}. \quad (7.37)$$

Substituting $x = y/\lambda^2$ into the closed form (7.9) gives

$$P_M^{(\lambda)}\left(\frac{y}{\lambda^2}\right) = \sum_{\substack{r,s \geq 0 \\ 2r+3s \leq M+1}} (-y)^{r+s} \lambda^{-2r} \binom{M+1-r-2s}{r+s} \binom{r+s}{r}. \quad (7.38)$$

Therefore only the terms with $r = 0$ survive, and we obtain the polynomial of the original FFD model [7]

$$R_M(y) := \lim_{\lambda \rightarrow \infty} P_M^{(\lambda)}\left(\frac{y}{\lambda^2}\right) = \sum_{\substack{s \geq 0 \\ 3s \leq M+1}} (-y)^s \binom{M+1-2s}{s}. \quad (7.39)$$

Equivalently, taking the same limit in the recursion and in the generating function gives

$$R_M(y) = R_{M-1}(y) - yR_{M-3}(y), \quad R_0 = 1, \quad R_1 = 1, \quad R_2 = 1 - y, \quad (7.40)$$

and

$$\sum_{M \geq 0} R_M(y) t^M = \frac{1 - yt^2}{1 - t + yt^3}. \quad (7.41)$$

Thus the finite roots of R_M describe precisely the modes for which $x = O(\lambda^{-2})$, or equivalently $\varepsilon = O(\lambda)$. The degree of R_M is $\lfloor (M+1)/3 \rfloor$; the remaining roots of $P_M^{(\lambda)}$ are sent to $y = \infty$ and therefore have $\widehat{\varepsilon} \rightarrow 0$ in this scaling.

We now obtain the limiting dispersion by taking $\lambda \rightarrow \infty$ in the finite- λ branch. For the linearly growing modes, the momentum remains in the interval $0 < p < \pi/3$; we denote it by θ . Put

$$c = \cos \theta, \quad q = 4c^2 - 1 > 0.$$

The large- λ expansion of (7.13) is

$$U_\lambda(\theta) = \frac{4c^2}{q} - \frac{4c^2}{q^3} \lambda^{-2} + O(\lambda^{-4}). \quad (7.42)$$

Consequently

$$U_\infty(\theta) = \frac{4 \cos^2 \theta}{4 \cos^2 \theta - 1}, \quad B_\infty(\theta) = \frac{2 \cos \theta}{4 \cos^2 \theta - 1} = \frac{\sin 2\theta}{\sin 3\theta}. \quad (7.43)$$

Taking the same limit in (7.14) gives

$$\lambda^2 x_\lambda(\theta) = \frac{4c^2}{q^3} \left[1 - \frac{2(1+2c^2)}{q^2} \lambda^{-2} + O(\lambda^{-4}) \right]. \quad (7.44)$$

Hence

$$y_\infty(\theta) = \frac{4 \cos^2 \theta}{(4 \cos^2 \theta - 1)^3}, \quad \widehat{\varepsilon}_\infty(\theta) = \frac{1}{\sqrt{y_\infty(\theta)}} = \frac{(4 \cos^2 \theta - 1)^{3/2}}{2 \cos \theta}, \quad 0 < \theta < \frac{\pi}{3}. \quad (7.45)$$

Equivalently,

$$\frac{\varepsilon_\lambda(\theta)}{\lambda} \rightarrow \frac{(4 \cos^2 \theta - 1)^{3/2}}{2 \cos \theta}. \quad (7.46)$$

This is Fendley's $q = 0$ FFD dispersion after identifying his momentum as $p_{\text{Fen}} = 3\theta$ [7]. The first correction follows from (7.44):

$$\frac{\varepsilon_\lambda(\theta)}{\lambda} = \frac{(4 \cos^2 \theta - 1)^{3/2}}{2 \cos \theta} \left[1 + \frac{1 + 2 \cos^2 \theta}{(4 \cos^2 \theta - 1)^2} \lambda^{-2} + O(\lambda^{-4}) \right]. \quad (7.47)$$

The limit is non-uniform at $\theta = \pi/3$. For fixed $p \in (\pi/3, \pi/2)$, put $d = 1 - 4 \cos^2 p > 0$. The same finite- λ formula gives

$$U_\lambda(p) = \lambda^2 d + d^{-1} + O(\lambda^{-2}), \quad (7.48)$$

and therefore

$$\varepsilon_\lambda(p) = \frac{2 \cos p}{\lambda^2 (1 - 4 \cos^2 p)^{3/2}} (1 + O(\lambda^{-2})). \quad (7.49)$$

This part of the physical branch collapses to zero energy in the scaled Hamiltonian H/λ . At the boundary $p = \pi/3$ one instead finds

$$\varepsilon_\lambda(\pi/3) \sim \lambda^{-1/2}. \quad (7.50)$$

It remains to take the same limit in the finite-size standing-wave formula. From (7.18) we obtain

$$\rho_\infty(\theta) = \frac{\sqrt{8 \cos^2 \theta + 1}}{4 \cos^2 \theta - 1}, \quad \delta_\infty(\theta) = \arctan \frac{2 \cos \theta \sin \theta}{2 \cos^2 \theta + 1}. \quad (7.51)$$

Taking $\lambda \rightarrow \infty$ in (7.19) gives the exact limiting phase formula

$$R_M(y_\infty(\theta)) = \frac{B_\infty(\theta)^{M+2}}{\rho_\infty(\theta) \sin \theta} \sin((M+3)\theta - \delta_\infty(\theta)) + \frac{(1 - U_\infty(\theta))^{M+3}}{\rho_\infty(\theta)^2}. \quad (7.52)$$

Therefore the exact limiting root condition is

$$\sin((M+3)\theta_\ell - \delta_\infty(\theta_\ell)) = -\frac{(1 - U_\infty(\theta_\ell))^{M+3} \sin \theta_\ell}{\rho_\infty(\theta_\ell) B_\infty(\theta_\ell)^{M+2}}, \quad \ell = 1, \dots, \left\lfloor \frac{M+1}{3} \right\rfloor. \quad (7.53)$$

Since

$$\left| \frac{1 - U_\infty(\theta)}{B_\infty(\theta)} \right| = \frac{1}{2 \cos \theta} < 1 \quad (0 < \theta < \pi/3), \quad (7.54)$$

the large- M standing-wave condition is

$$(M+3)\theta_\ell - \delta_\infty(\theta_\ell) = \pi\ell + O\left((2 \cos \theta_\ell)^{-(M+2)}\right), \quad \ell = 1, \dots, \left\lfloor \frac{M+1}{3} \right\rfloor. \quad (7.55)$$

8 Conclusions

In this work we presented a spin-chain model that falls under the broad umbrella of “free fermions in disguise” and is free from exponential degeneracies. In Subsection 4.2 we explained why it is difficult to find such a model. We now summarize the mechanism that makes these special properties possible.

In our case the final Hamiltonian is a combination of two Hamiltonians H_1 and H_2 . Both have $2M - 1$ terms, where M is the size of a fundamental graph-Clifford algebra. Thus, we have a total of $4M - 2$ generators. However, they are not independent, and there are $2M - 2$ independent algebraic relations between them. As a result, the combined generator set can be represented on $M + \mathcal{O}(1)$ qubits. At the same time, the frustration graphs of the two Hamiltonians H_1 and H_2 allow for $\lfloor (M + 1)/2 \rfloor$ fermionic eigenmodes, leading to a total of $2\lfloor (M + 1)/2 \rfloor$ eigenmodes. Thus, we have enough eigenmodes to avoid exponential degeneracies.

However, there is an additional crucial point: even though H_1 and H_2 have ECF-type frustration graphs, this is not true for the combined generator set. Consequently, the model would not even be integrable for arbitrary coupling constants in the combined generator set. If we choose the couplings such that special quadratic relations are satisfied, then we obtain the necessary cancellations that ensure commutativity of H_1 and H_2 and the compatibility of their free-fermionic structures. Such relations were used in the work [12] for a single Hamiltonian. In our case we can find the relations for the combined generator set of two Hamiltonians H_1 and H_2 , thereby avoiding the exponential degeneracies.

Our Hamiltonian $H_1 - H_2$ in the XY representation is structurally appealing: it interpolates between the $U(1)$ -invariant XY model (given by the Dzyaloshinskii–Moriya interaction term) and the original FFD model of Fendley. The degeneracies are constant along the line connecting the two models, except for the FFD endpoint, which corresponds to $\lambda = \infty$ in our conventions. For numerical data about the interpolation, see Appendix A.2.

Given that our model is a perturbation of a Jordan-Wigner solvable model, and that the free-fermionic operators change continuously with λ , a natural question is whether there is any sort of “simple” connection between the models. Is there perhaps a finite-depth quantum circuit or an MPO with finite bond dimension that could connect the structures of the FFD-type perturbation and the XY chain? If such a circuit or MPO exists, it would suggest that even the original FFD model can be obtained from the XY chain by such “simple” means. Currently it is not known whether such a connection can or cannot exist.

We also note an interesting observation: If we apply the standard techniques of integrable models to the transfer matrices, then we can define appropriate Lax operators and also R -matrices that perform intertwining steps. Interestingly, we find that the R -matrix of the model is exactly the same 9×9 matrix for all (inhomogeneous) coupling constants. This includes the FFD model itself as an endpoint of the interpolation. A simplification arises only in the XY endpoint, where only a 4×4 block of the R -matrix remains relevant. These results are not used in our main derivations, but they are presented as complementary material in Appendix C. Results about the integrability structures may be relevant to the study of the models with periodic boundary conditions.

In future work we plan to investigate other mechanisms that lead to non-degenerate FFD-type models. As we were preparing this manuscript, we discovered another such model with a related but slightly different mechanism. We leave this topic to further research.

Acknowledgements

We thank Kohei Fukai and István Vona for many useful discussions and collaborations on related topics. We also thank István Vona for an independent AI-based check of the results of this work.

The author was supported by the Hungarian National Research, Development and Innovation Office, NKFIH Grant No. K-145904.

A Numerical data

A.1 Free fermions for $H_1 - H_2$

We now give a direct numerical check of the spectral formulas in the XY representation. We restrict to the combination $H_1 - H_2$ and choose

$$\lambda = 1, \quad \beta_k = \sin k, \quad \tilde{\beta}_k = \cos k, \quad k = 1, \dots, M,$$

where the argument of the trigonometric functions is measured in radians. For our purposes these couplings serve as completely generic numbers.

For these parameters we diagonalize the Pauli-chain Hamiltonian

$$H_1 - H_2 = \sum_{j=1}^M \left(\beta_j Y_j X_{j+1} - \tilde{\beta}_j X_j Y_{j+1} \right) + \sum_{j=1}^{M-1} \left(\alpha_j Z_j X_{j+1} X_{j+2} - \tilde{\alpha}_j X_j X_{j+1} Z_{j+2} \right),$$

with

$$\alpha_j = \beta_j \beta_{j+1} \tilde{\beta}_j, \quad \tilde{\alpha}_j = \tilde{\beta}_j \tilde{\beta}_{j+1} \beta_{j+1}.$$

The chain length in the XY representation is

$$L = M + 1,$$

so the exact diagonalization is performed on a Hilbert space of dimension 2^L .

The energies obtained from the free-fermionic solution are compared with the sign-sum expression (5.18).

The common multiplicity in the XY representation is

$$2^{L-2S}.$$

The one-particle energies are extracted from the spectral polynomials

$$P_{a,M}(x) = \prod_{r=1}^S (1 - \varepsilon_{a,r}^2 x), \quad a = 1, 2.$$

For the two tested system sizes the resulting polynomials are given in Table 1.

The corresponding positive one-particle energies are listed in Table 2. These are the numbers entering the sign-sum expression above.

We next list the resulting exact-diagonalization spectrum of $H_1 - H_2$. Only positive energies are shown; the spectrum is symmetric under $E \mapsto -E$. For $M = 4$, every listed positive energy and its

Table 1: Spectral polynomials for $M = 4, 5$.

M	Polynomial	$P_{a,M}(x)$
4	$P_{1,4}$	$1 - 2.312499318432 x + 0.999015949013 x^2$
4	$P_{2,4}$	$1 - 2.157454394006 x + 0.572702017908 x^2$
5	$P_{1,5}$	$1 - 3.457052321338 x + 2.972333349787 x^2 - 0.012966539921 x^3$
5	$P_{2,5}$	$1 - 2.269530745604 x + 0.708647863841 x^2 - 0.023021856212 x^3$

Table 2: Positive one-particle energies.

M	Sector	$\varepsilon_{a,1}$	$\varepsilon_{a,2}$	$\varepsilon_{a,3}$
4	$a = 1$	0.758261362983	1.318157435149	–
4	$a = 2$	0.556771270364	1.359213061482	–
5	$a = 1$	0.066217399570	1.254816328025	1.370439185172
5	$a = 2$	0.191676889058	0.573733517849	1.379717567585

negative partner have multiplicity 2, in agreement with $2^{L-2S} = 2$. For $M = 5$, all levels are simple, in agreement with $2^{L-2S} = 1$.

The agreement between exact diagonalization and the sign-sum construction is at the level of numerical roundoff in both examples. No accidental degeneracies are observed in these two tests. The only degeneracy for $M = 4$ is the uniform twofold multiplicity in the XY representation $2^{L-2S} = 2$, while for $M = 5$ the full spectrum is non-degenerate.

A.2 The change in the degeneracy pattern

Here we display the change in the degeneracy pattern as we move from the XY point to the FFD point. To do this, we choose $M = 4$, random β_k and $\tilde{\beta}_k$ couplings, and vary λ from zero to infinity. To keep the spectra finite, we renormalize the Hamiltonian and present data for the spectrum of

$$H_\theta \equiv \cos(\theta)H_0 + \sin(\theta)H_{FFD}, \quad (\text{A.1})$$

where

$$H_0 = \sum_{j=1}^M B_j - \tilde{B}_j, \quad H_{FFD} = \sum_{j=1}^{M-1} A_j - \tilde{A}_j. \quad (\text{A.2})$$

We performed exact diagonalization and present spectral data for $\theta \in [0, \pi/2]$. The random couplings are shown in Table 5. For reference, we present concrete numerical values for the energies at $\theta = 0$ and $\theta = \pi/2$ in Table 6. Finally, the spectrum is plotted in Fig. 4.

B Factorization of the transfer matrix

Here we prove that simple factorized formulas exist for the transfer matrices $T_{1,2}(u)$, analogous to the one originally derived in [7].

Consider now a single Hamiltonian of the form

$$H = \sum_{j=1}^{M-1} A_j + \sum_{j=1}^M B_j, \quad (\text{B.1})$$

Table 3: Positive exact-diagonalization energies of $H_1 - H_2$ for $M = 4$. Each listed energy and its negative partner have multiplicity 2.

$M = 4$			
0.160434466286	0.242545718951	1.273977007015	1.356088259680
1.362337863284	2.475880404013	2.878860589250	3.992403129979

Table 4: Positive exact-diagonalization energies of $H_1 - H_2$ for $M = 5$. All listed energies and their negative partners are simple.

$M = 5$			
0.413910139136	0.432466903961	0.546344938275	0.564901703101
0.663712618255	0.796147417394	0.797263917252	0.815820682077
0.929698716391	0.948255481217	1.047066396370	1.179501195510
1.561377174834	1.579933939660	1.693811973973	1.712368738799
1.811179653953	1.943614453092	1.944730952950	1.963287717775
2.077165752089	2.095722516915	2.194533432068	2.326968231208
3.173345274305	3.305780073444	3.556699052421	3.689133851560
4.320812310003	4.453247109142	4.704166088119	4.836600887258

where the generators obey the interval anti-commutation pattern of one chain and have scalar squares

$$A_j^2 = \alpha_j^2 \mathbf{1}, \quad B_j^2 = \beta_j^2 \mathbf{1}. \quad (\text{B.2})$$

For non-zero weights set $\hat{A}_j = A_j/\alpha_j$ and $\hat{B}_j = B_j/\beta_j$. Its transfer matrix is

$$T_M(u) = \sum_{S \in \mathcal{I}_M} (-u)^{|S|} \prod_{A_j \in S} A_j \prod_{B_k \in S} B_k. \quad (\text{B.3})$$

The order is immaterial inside each independent set, because the selected generators commute. The same right-boundary decomposition used in the main text gives

$$T_m(u) = T_{m-1}(u) - uB_m T_{m-2}(u) - uA_{m-1} T_{m-3}(u), \quad m \geq 2, \quad (\text{B.4})$$

with

$$T_{-1}(u) = T_0(u) = \mathbf{1}, \quad T_1(u) = \mathbf{1} - uB_1. \quad (\text{B.5})$$

Indeed, an independent set for the prefix with short generators B_1, \dots, B_m either contains no generator touching the right boundary, contains B_m , or contains A_{m-1} . In the last two cases the remaining part lies in the prefixes of lengths $m - 2$ and $m - 3$, respectively. For $m = 2$ this gives

$$T_2(u) = \mathbf{1} - u(B_1 + B_2 + A_1),$$

as required.

Define, for any involution $O^2 = \mathbf{1}$,

$$g(O, \phi) = \cos \frac{\phi}{2} + O \sin \frac{\phi}{2}. \quad (\text{B.6})$$

Choose the angles recursively by

$$\phi_{-1}^A = \phi_0^A = \phi_0^B = 0, \quad \sin \phi_1^B = -u \beta_1, \quad (\text{B.7})$$

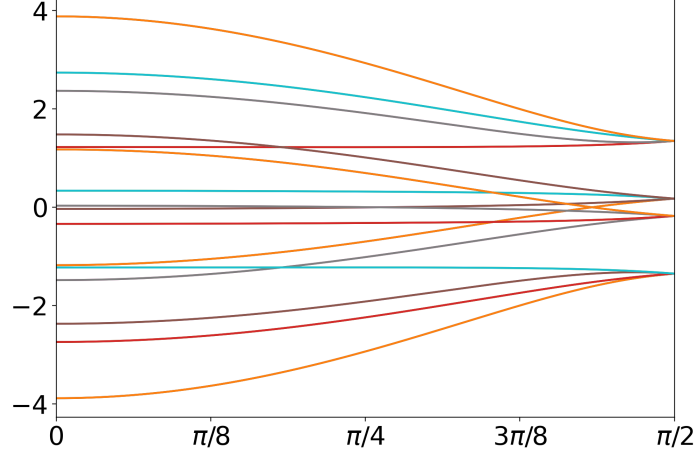


Figure 4: The spectrum of H_θ as a function of θ , for $M = 4$. For each value of $\theta \neq \pi/2$ there are 16 different eigenvalues, each with a homogeneous degeneracy of 2, corresponding to the chain having length $L = M + 1 = 5$. They collapse to 4 eigenvalues at $\theta = \pi/2$, corresponding to the FFD model, which has $\mathcal{S} = 2$ eigenmodes for $M = 4$.

Table 5: Random couplings used for the $M = 4$ interpolation.

k	β_k	$\tilde{\beta}_k$
1	0.773956048556	0.094177347888
2	0.438878439752	0.975622351637
3	0.858597919911	0.761139701990
4	0.697368029059	0.786064305277

$$\sin \phi_j^A = -\frac{u \alpha_j}{\cos \phi_{j-2}^A \cos \phi_{j-1}^B \cos \phi_{j-1}^A \cos \phi_j^B}, \quad 1 \leq j \leq M-1, \quad (\text{B.8})$$

$$\sin \phi_{j+1}^B = -\frac{u \beta_{j+1}}{\cos \phi_j^A \cos \phi_{j-1}^A \cos \phi_j^B}, \quad 1 \leq j \leq M-1. \quad (\text{B.9})$$

The angles are well-defined at least in a neighbourhood of $u = 0$ and can then be continued analytically.

With

$$g_j^A = \cos \frac{\phi_j^A}{2} + \hat{A}_j \sin \frac{\phi_j^A}{2}, \quad g_j^B = \cos \frac{\phi_j^B}{2} + \hat{B}_j \sin \frac{\phi_j^B}{2}, \quad (\text{B.10})$$

$$G_M = g_1^B g_1^A g_2^B g_2^A \cdots g_{M-1}^B g_{M-1}^A g_M^B, \quad (\text{B.11})$$

and

$$G_M^{\text{rev}} = g_M^B g_{M-1}^A g_{M-1}^B \cdots g_1^A g_1^B, \quad (\text{B.12})$$

one obtains the exact factorization

$$T_M(u) = G_M(u) G_M^{\text{rev}}(u). \quad (\text{B.13})$$

The proof is an algebraic induction based on (B.4) and the elementary identities

$$g(O, \phi)^2 = \mathbf{1} + O \sin \phi, \quad g(O, \phi) X g(O, \phi) = \begin{cases} (\cos \phi) X, & \{O, X\} = 0, \\ X(\mathbf{1} + O \sin \phi), & [O, X] = 0. \end{cases} \quad (\text{B.14})$$

Table 6: Spectra of the Hamiltonians H_θ at $\theta = 0$ and $\theta = \pi/2$, for $M = 4$. Only positive energies are listed; the spectrum is symmetric under $E \mapsto -E$. At $\theta = 0$, each listed positive level and its negative partner are twofold degenerate. At $\theta = \pi/2$, each listed positive level and its negative partner are eightfold degenerate.

Endpoint	Positive energies $E > 0$
$\theta = 0$	0.032944896137
	0.337604621603
	1.176669844980
	1.224894658396
	1.481329570446
	2.368619607239
	2.739169124980
	3.882894073823
$\theta = \pi/2$	0.176626910954
	1.349446176826

They follow by writing $g(O, \phi) = c + sO$, with $c = \cos(\phi/2)$ and $s = \sin(\phi/2)$. Then $(c + sO)^2 = \mathbf{1} + 2csO = \mathbf{1} + O \sin \phi$. If $XO = -OX$, then $(c + sO)X = X(c - sO)$, giving $g(O, \phi)Xg(O, \phi) = X(c^2 - s^2)$. If $XO = OX$, then X can be moved through both factors and the first identity applies.

For the induction, set

$$F_m(u) = G_m(u)G_m^{\text{rev}}(u), \quad F_{-1}(u) = F_0(u) = \mathbf{1}. \quad (\text{B.15})$$

For $m = 1$,

$$F_1(u) = (g_1^B)^2 = \mathbf{1} + \widehat{B}_1 \sin \phi_1^B = \mathbf{1} - u\beta_1 \widehat{B}_1 = \mathbf{1} - uB_1 = T_1(u).$$

For $m \geq 2$ one has

$$G_m = G_{m-1}g_{m-1}^A g_m^B, \quad G_m^{\text{rev}} = g_m^B g_{m-1}^A G_{m-1}^{\text{rev}}.$$

Using (B.14),

$$\begin{aligned} F_m &= G_{m-1}g_{m-1}^A (g_m^B)^2 g_{m-1}^A G_{m-1}^{\text{rev}} \\ &= F_{m-1} + \sin \phi_{m-1}^A G_{m-1} \widehat{A}_{m-1} G_{m-1}^{\text{rev}} \\ &\quad + \sin \phi_m^B \cos \phi_{m-1}^A G_{m-1} \widehat{B}_m G_{m-1}^{\text{rev}}. \end{aligned} \quad (\text{B.16})$$

The operator \widehat{A}_{m-1} anti-commutes exactly with g_{m-3}^A , g_{m-2}^B , g_{m-2}^A , and g_{m-1}^B inside G_{m-1} , with the convention that gates with non-positive indices are absent. It commutes with all other gates. Therefore

$$G_{m-1} \widehat{A}_{m-1} G_{m-1}^{\text{rev}} = \cos \phi_{m-3}^A \cos \phi_{m-2}^B \cos \phi_{m-2}^A \cos \phi_{m-1}^B \widehat{A}_{m-1} F_{m-3}. \quad (\text{B.17})$$

Similarly, \widehat{B}_m anti-commutes exactly with g_{m-2}^A and g_{m-1}^B inside G_{m-1} , and hence

$$G_{m-1} \widehat{B}_m G_{m-1}^{\text{rev}} = \cos \phi_{m-2}^A \cos \phi_{m-1}^B \widehat{B}_m F_{m-2}. \quad (\text{B.18})$$

Substituting (B.17) and (B.18) into (B.16), and then using (B.8) and (B.9), gives

$$F_m(u) = F_{m-1}(u) - uA_{m-1}F_{m-3}(u) - uB_m F_{m-2}(u). \quad (\text{B.19})$$

This is the recursion (B.4), with the same initial data (B.5). Hence $F_m(u) = T_m(u)$ for every m , and in particular (B.13) holds for $m = M$.

C MPO representations in the XY representation

In this appendix we give a self-contained MPO construction for either the H_1 or the H_2 family in the XY representation. These MPOs are not used in any of the proofs in the main text; instead we present them to complement the material. We note that for the fermionic operators we find an MPO of bond dimension 4, and this is a new result even for the FFD model of Fendley. The results below are valid for every spectral parameter u , and not only the “on-shell” ones.

We use L for the length of the Pauli chain and $M = L - 1$ for the number of B -generators. For simplicity we focus only on H_1 and write

$$H = \sum_{j=1}^M B_j + \sum_{j=1}^{M-1} A_j, \quad B_j = \beta_j Y_j X_{j+1}, \quad A_j = \alpha_j Z_j X_{j+1} X_{j+2}. \quad (\text{C.1})$$

Here $j = 1, \dots, M$ for B_j and $j = 1, \dots, M - 1$ for A_j . We use the boundary convention

$$\beta_j = 0 \quad (j \notin \{1, \dots, M\}), \quad \alpha_j = 0 \quad (j \notin \{1, \dots, M - 1\}). \quad (\text{C.2})$$

In particular $\beta_L = 0$, $\alpha_M = 0$, and $\alpha_L = 0$.

For $0 \leq m \leq M$, let \mathcal{I}_m be the independent sets of the interval family

$$B_j \leftrightarrow [j, j + 1], \quad A_j \leftrightarrow [j, j + 2], \quad 1 \leq j \leq m, \quad 1 \leq j \leq m - 1 \quad (\text{C.3})$$

on the prefix with m short generators. Thus the corresponding physical prefix has $m + 1$ sites. For $S \in \mathcal{I}_m$, let $g(S)$ be the ordered product of the selected generators, ordered by increasing left endpoint. The order is immaterial inside an independent set, because the selected generators commute. We define

$$T_m(u) = \sum_{S \in \mathcal{I}_m} (-u)^{|S|} g(S), \quad 0 \leq m \leq M. \quad (\text{C.4})$$

The full transfer matrix of the chain is $T_M(u)$, and

$$-\partial_u T_M(0) = H. \quad (\text{C.5})$$

C.1 Bond-dimension-3 MPO for the transfer matrix

Introduce a three-dimensional auxiliary space with basis $|0\rangle, |1\rangle, |2\rangle$, and let E_{rs} be its matrix units. The local Lax operator is

$$\mathcal{L}_j(u) = E_{00} \otimes \mathbf{1}_j - u\beta_j E_{01} \otimes Y_j - u\alpha_j E_{02} \otimes Z_j + E_{10} \otimes X_j + E_{21} \otimes X_j. \quad (\text{C.6})$$

Equivalently,

$$\mathcal{L}_j(u) = \begin{pmatrix} \mathbf{1}_j & -u\beta_j Y_j & -u\alpha_j Z_j \\ X_j & 0 & 0 \\ 0 & X_j & 0 \end{pmatrix}. \quad (\text{C.7})$$

Then

$$T_M(u) = \langle 0 | \mathcal{L}_1(u) \mathcal{L}_2(u) \cdots \mathcal{L}_L(u) | 0 \rangle. \quad (\text{C.8})$$

The auxiliary interpretation is that state 0 means that no X -operator is pending, state 1 records one pending X , and state 2 records two pending X 's. The transition

$$0 \xrightarrow{-u\beta_j Y_j} 1 \xrightarrow{X_{j+1}} 0$$

produces the tile $-uB_j$, while

$$0 \xrightarrow{-u\alpha_j Z_j} 2 \xrightarrow{X_{j+1}} 1 \xrightarrow{X_{j+2}} 0$$

produces the tile $-uA_j$. Thus the MPO is an automaton for non-overlapping tiles of lengths 2 and 3.

Setting $\beta_j = 0$ in (C.7) we obtain the Lax operators that were found by Fendley in [7].

Proposition C.1. *The MPO formula (C.8) reproduces the independent-set transfer matrix (C.4).*

Proof. For $0 \leq n \leq L$, define the partial contractions

$$F_n^{(r)}(u) = \langle 0 | \mathcal{L}_1(u) \cdots \mathcal{L}_n(u) | r \rangle, \quad r = 0, 1, 2, \quad (\text{C.9})$$

with $F_0^{(0)} = \mathbf{1}$ and $F_0^{(1)} = F_0^{(2)} = 0$. From (C.7),

$$F_n^{(0)} = F_{n-1}^{(0)} + F_{n-1}^{(1)} X_n, \quad (\text{C.10})$$

$$F_n^{(1)} = -u\beta_n F_{n-1}^{(0)} Y_n + F_{n-1}^{(2)} X_n, \quad (\text{C.11})$$

$$F_n^{(2)} = -u\alpha_n F_{n-1}^{(0)} Z_n. \quad (\text{C.12})$$

Eliminating $F^{(1)}$ and $F^{(2)}$ gives, for $n \geq 3$,

$$F_n^{(0)} = F_{n-1}^{(0)} - uB_{n-1} F_{n-2}^{(0)} - uA_{n-2} F_{n-3}^{(0)}. \quad (\text{C.13})$$

The initial values are

$$F_0^{(0)} = \mathbf{1}, \quad F_1^{(0)} = \mathbf{1}, \quad F_2^{(0)} = \mathbf{1} - uB_1. \quad (\text{C.14})$$

On the other hand, the independent-set transfer matrices satisfy

$$T_m(u) = T_{m-1}(u) - uB_m T_{m-2}(u) - uA_{m-1} T_{m-3}(u), \quad (\text{C.15})$$

with $T_{-1}(u) = T_0(u) = \mathbf{1}$ and with $A_0 = 0$. This follows by splitting an independent set according to the right boundary: it either contains no generator touching the right endpoint, or it contains B_m , or it contains A_{m-1} . Comparing (C.13) with (C.15) gives

$$F_n^{(0)}(u) = T_{n-1}(u).$$

Setting $n = L = M + 1$ proves (C.8). □

C.2 RTT relation

The local Lax operator admits a site-independent auxiliary R -matrix. Let

$$\begin{aligned} \mathcal{R}(u, v) = & (u + v) \sum_{i=0}^2 E_{ii} \otimes E_{ii} + (v - u) \sum_{0 \leq i < j \leq 2} E_{ii} \otimes E_{jj} + (u - v) \sum_{0 \leq i < j \leq 2} E_{jj} \otimes E_{ii} \\ & + 2u \sum_{0 \leq i < j \leq 2} E_{ij} \otimes E_{ji} + 2v \sum_{0 \leq i < j \leq 2} E_{ji} \otimes E_{ij}. \end{aligned} \quad (\text{C.16})$$

Then we find the following remarkable identity:

$$\mathcal{R}_{12}(u, v) \mathcal{L}_{1j}(u) \mathcal{L}_{2j}(v) = \mathcal{L}_{2j}(v) \mathcal{L}_{1j}(u) \mathcal{R}_{12}(u, v). \quad (\text{C.17})$$

The subscripts 1, 2 refer to the two auxiliary spaces.

We stress that $R_{12}(u, v)$ does not depend on the inhomogeneities, but the Lax operators explicitly depend on β_j and α_j . In the special case $\beta_j = 0$ we obtain the RLL relation derived by Fendley in [7]. Thus, from the integrability point of view, the whole model family belongs to the same integrable structure, and only the Lax operator changes as we switch on the perturbation.

The verification of the RLL relation uses only the Pauli identities

$$X_j Y_j = iZ_j, \quad Y_j X_j = -iZ_j, \quad Z_j X_j = iY_j, \quad X_j Z_j = -iY_j, \quad (\text{C.18})$$

together with $X_j^2 = Y_j^2 = Z_j^2 = \mathbf{1}_j$. After substituting (C.7), both sides of (C.17) are 9×9 auxiliary matrices whose entries are linear combinations of $\mathbf{1}_j, X_j, Y_j, Z_j$; comparing these four coefficients entry by entry gives (C.17).

Multiplying (C.17) over $j = 1, \dots, L$ gives the global RTT relation for

$$\Omega(u) = \mathcal{L}_1(u) \mathcal{L}_2(u) \cdots \mathcal{L}_L(u).$$

Since

$$\mathcal{R}(u, v)|00\rangle = (u + v)|00\rangle, \quad \langle 00|\mathcal{R}(u, v) = (u + v)\langle 00|,$$

sandwiching the global RTT relation between $\langle 00|$ and $|00\rangle$ gives

$$[T_M(u), T_M(v)] = 0. \quad (\text{C.19})$$

For $u + v = 0$ the same identity follows by polynomial continuation.

C.3 The dressed edge operator

The right boundary Pauli operator

$$\chi_R = Z_L \quad (\text{C.20})$$

anti-commutes precisely with B_M and A_{M-1} , and commutes with all other B_j, A_j . The dressed edge operator is

$$\Psi_L(u) = T_M(-u) Z_L T_M(u). \quad (\text{C.21})$$

At a zero $u = u_k$ of the scalar polynomial associated with $T_M(-u)T_M(u)$, the operators $\Psi_L(\pm u_k)$ give the corresponding fermionic eigenmode operators after normalization.

For later use, set

$$x_j = u\beta_j, \quad y_j = u\alpha_j, \quad 1 \leq j \leq M, \quad (\text{C.22})$$

with $y_M = 0$. Define the scalar prefix polynomial $p_m(u)$ by

$$p_m(u) = \sum_{S \in \mathcal{I}_m} (-u^2)^{|S|} \prod_{g \in S} w(g)^2, \quad w(B_j) = \beta_j, \quad w(A_j) = \alpha_j. \quad (\text{C.23})$$

Equivalently,

$$p_{-1}(u) = p_0(u) = 1, \quad p_1(u) = 1 - x_1^2, \quad (\text{C.24})$$

and for $m \geq 2$,

$$p_m(u) = p_{m-1}(u) - x_m^2 p_{m-2}(u) - y_{m-1}^2 p_{m-3}(u). \quad (\text{C.25})$$

Thus $p_M(u)$ is the full scalar polynomial, written as a polynomial in u^2 .

C.4 Naive doubled MPO and the final-site boundary

Starting from (C.8), the naive doubled MPO for $\Psi_L(u)$ has auxiliary dimension 9. For $1 \leq j \leq M$, define

$$\mathcal{K}_j(u) = \mathcal{L}_j(-u) \otimes \mathcal{L}_j(u). \quad (\text{C.26})$$

The tensor product is over the two auxiliary spaces, while the physical entries are multiplied in the order in which they appear in $T_M(-u)Z_L T_M(u)$.

The last physical site is more naturally kept as a right boundary vector, because Z_L sits between the two final Lax factors. In the standard basis $|a\rangle \otimes |b\rangle$, $0 \leq a, b \leq 2$, define

$$(|r_9(u)\rangle)_{ab} = (\mathcal{L}_L(-u))_{a0} Z_L (\mathcal{L}_L(u))_{b0}. \quad (\text{C.27})$$

Since $\beta_L = \alpha_L = 0$, the only nonzero entries are

$$(r_9)_{00} = Z_L, \quad (r_9)_{11} = -Z_L, \quad (r_9)_{01} = iY_L, \quad (r_9)_{10} = -iY_L. \quad (\text{C.28})$$

Then

$$\Psi_L(u) = \langle 00 | \mathcal{K}_1(u) \mathcal{K}_2(u) \cdots \mathcal{K}_M(u) | r_9(u) \rangle. \quad (\text{C.29})$$

C.5 Exact compression from bond dimension 9 to 6

Let $\mathcal{W}_6 \subset \mathbb{C}^3 \otimes \mathbb{C}^3$ be spanned by

$$\begin{aligned} s_1 &= |00\rangle, & s_2 &= |11\rangle, & s_3 &= |22\rangle, \\ s_4 &= \frac{|20\rangle - |02\rangle}{2}, & s_5 &= \frac{|10\rangle - |01\rangle}{2}, & s_6 &= \frac{|21\rangle - |12\rangle}{2}. \end{aligned} \quad (\text{C.30})$$

The factors 1/2 are a basis convention chosen so that the reduced tensor has no extra factors 1/2. With row-vector multiplication, a direct local calculation gives

$$\begin{aligned} s_1 \mathcal{K}_j &= s_1 - x_j^2 s_2 - y_j^2 s_3 + 2y_j Z_j s_4 + 2x_j Y_j s_5 + 2ix_j y_j X_j s_6, \\ s_2 \mathcal{K}_j &= s_1, \\ s_3 \mathcal{K}_j &= s_2, \\ s_4 \mathcal{K}_j &= X_j s_5 - iy_j Y_j s_6, \\ s_5 \mathcal{K}_j &= -iy_j Y_j s_4 + ix_j Z_j s_5, \\ s_6 \mathcal{K}_j &= s_5. \end{aligned} \quad (\text{C.31})$$

Hence \mathcal{W}_6 is invariant under every $\mathcal{K}_j(u)$. Moreover, $|00\rangle = s_1$ and the boundary vector $|r_9(u)\rangle$ belongs to \mathcal{W}_6 . In the basis (C.30), the reduced local tensor is

$$\mathbf{M}_j^{(6)}(u) = \begin{pmatrix} \mathbf{1}_j & -x_j^2 \mathbf{1}_j & -y_j^2 \mathbf{1}_j & 2y_j Z_j & 2x_j Y_j & 2ix_j y_j X_j \\ \mathbf{1}_j & 0 & 0 & 0 & 0 & 0 \\ 0 & \mathbf{1}_j & 0 & 0 & 0 & 0 \\ 0 & 0 & 0 & 0 & X_j & -iy_j Y_j \\ 0 & 0 & 0 & -iy_j Y_j & ix_j Z_j & 0 \\ 0 & 0 & 0 & 0 & \mathbf{1}_j & 0 \end{pmatrix}. \quad (\text{C.32})$$

The reduced right boundary is

$$|r_6(u)\rangle = \begin{pmatrix} Z_L \\ -Z_L \\ 0 \\ 0 \\ -iY_L \\ 0 \end{pmatrix}, \quad \langle \ell_6 | = (1, 0, 0, 0, 0, 0). \quad (\text{C.33})$$

Therefore

$$\Psi_L(u) = \langle \ell_6 | \mathbf{M}_1^{(6)}(u) \mathbf{M}_2^{(6)}(u) \cdots \mathbf{M}_M^{(6)}(u) | r_6(u) \rangle. \quad (\text{C.34})$$

C.6 Exact compression from bond dimension 6 to 4

The tensor $\mathbf{M}_j^{(6)}(u)$ is block upper triangular. Its first three states form a scalar block,

$$S_j(u) = \begin{pmatrix} 1 & -x_j^2 & -y_j^2 \\ 1 & 0 & 0 \\ 0 & 1 & 0 \end{pmatrix}. \quad (\text{C.35})$$

Starting from the scalar row vector $(1, 0, 0)$, the first component after r sites is $p_{r-1}(u)$. In particular, before site j the first scalar component is $p_{j-2}(u)$. Since the coupling from the scalar block to the non-scalar block occurs only from the first scalar state, we can integrate out the scalar block exactly.

The resulting bond-dimension-4 tensor acts on the basis consisting of one integrated scalar state, followed by s_4, s_5, s_6 . In the following display p_{j-2} means $p_{j-2}(u)$, with $p_{-1}(u) = p_0(u) = 1$:

$$\mathbf{M}_j^{(4)}(u) = \begin{pmatrix} \mathbf{1}_j & 2y_j p_{j-2} Z_j & 2x_j p_{j-2} Y_j & 2ix_j y_j p_{j-2} X_j \\ 0 & 0 & X_j & -iy_j Y_j \\ 0 & -iy_j Y_j & ix_j Z_j & 0 \\ 0 & 0 & \mathbf{1}_j & 0 \end{pmatrix}. \quad (\text{C.36})$$

It remains to compute the scalar part of the final boundary. After M sites, the scalar row has first component $p_{M-1}(u)$. If one appended the last zero-weight site $L = M + 1$, the new first component would be $p_M(u)$. Thus the second scalar component before the last site is $p_M(u) - p_{M-1}(u)$. Contracting with the scalar part $(Z_L, -Z_L, 0)^t$ of (C.33) gives

$$p_{M-1} Z_L - (p_M - p_{M-1}) Z_L = (2p_{M-1} - p_M) Z_L.$$

Therefore

$$|r_4(u)\rangle = \begin{pmatrix} (2p_{M-1}(u) - p_M(u)) Z_L \\ 0 \\ -iY_L \\ 0 \end{pmatrix}, \quad \langle \ell_4 | = (1, 0, 0, 0). \quad (\text{C.37})$$

The final compressed formula is

$$\Psi_L(u) = \langle \ell_4 | \mathbf{M}_1^{(4)}(u) \mathbf{M}_2^{(4)}(u) \cdots \mathbf{M}_M^{(4)}(u) | r_4(u) \rangle. \quad (\text{C.38})$$

The compressions

$$9 \longrightarrow 6 \longrightarrow 4$$

are exact for arbitrary inhomogeneous coefficients α_j, β_j .

To our knowledge, this MPO construction is new even for the original FFD model of Fendley.

References

- [1] P. Jordan and E. Wigner, “Über das Paulische Äquivalenzverbot,” *Z. Physik* **47** (1928) 631–651.
- [2] K. Minami, “Solvable Hamiltonians and Fermionization Transformations Obtained from Operators Satisfying Specific Commutation Relations,” *J. Phys. Soc. Japan* **85** (2016) no. 2, 024003.
- [3] K. Minami, “Infinite number of solvable generalizations of XY-chain, with cluster state, and with central charge $c = m/2$,” *Nucl. Phys. B* **925** (2017) 144–160, [arXiv:1710.01851 \[cond-mat.stat-mech\]](#).
- [4] Y. Yanagihara and K. Minami, “Exact solution of a cluster model with next-nearest-neighbor interaction,” *Progr. of Theor. Exp. Phys.* **2020** (2020) no. 11, 113A01, [arXiv:2003.00962 \[cond-mat.stat-mech\]](#).
- [5] M. Ogura, Y. Imamura, N. Kameyama, K. Minami, and M. Sato, “Geometric criterion for solvability of lattice spin systems,” *Phys. Rev. B* **102** (2020) no. 24, 245118, [arXiv:2003.13264 \[cond-mat.stat-mech\]](#).
- [6] A. Chapman and S. T. Flammia, “Characterization of solvable spin models via graph invariants,” *Quantum* **4** (2020) 278, [arXiv:2003.05465 \[quant-ph\]](#).
- [7] P. Fendley, “Free fermions in disguise,” *J. Phys. A* **52** (2019) no. 33, 335002, [arXiv:1901.08078 \[cond-mat.stat-mech\]](#).
- [8] S. J. Elman, A. Chapman, and S. T. Flammia, “Free fermions behind the disguise,” *Commun. Math. Phys.* **388** (2021) 969–1003, [arXiv:2012.07857 \[quant-ph\]](#).
- [9] K. Fukai, B. Pozsgay, and I. Vona, “Solving models with generalized free fermions II: Path-product expansion and conserved charges,” *arXiv e-prints* (2026) , [arXiv:2605.31453 \[cond-mat.stat-mech\]](#).
- [10] E. Vernier and L. Piroli, “The Hilbert-space structure of free fermions in disguise,” *JSTAT* **2026** (2026) no. 1, 013101, [arXiv:2507.15959 \[cond-mat.stat-mech\]](#).
- [11] K. Fukai, B. Pozsgay, and I. Vona, “Solving models with generalized free fermions I: Algebras and eigenstates,” *arXiv e-prints* (2026) , [arXiv:2602.03431 \[cond-mat.stat-mech\]](#).
- [12] P. Fendley and B. Pozsgay, “Free fermions beyond Jordan and Wigner,” *SciPost Physics* **16** (2024) no. 4, 102, [arXiv:2310.19897 \[cond-mat.stat-mech\]](#).
- [13] K. Fukai, I. Vona, and B. Pozsgay, “A free fermions in disguise model with claws,” *arXiv e-prints* (2025) , [arXiv:2508.05789 \[cond-mat.stat-mech\]](#).
- [14] A. Chapman, S. J. Elman, and R. L. Mann, “A Unified Graph-Theoretic Framework for Free-Fermion Solvability,” *arXiv e-prints* (2023) , [arXiv:2305.15625 \[quant-ph\]](#).
- [15] T. Khovanova, “Clifford Algebras and Graphs,” *Geombinatorics* **XX (2)** (2010) 56, [arXiv:0810.3322 \[math.CO\]](#).
- [16] K. Fukai and B. Pozsgay, “Quantum circuits with free fermions in disguise,” *J. Phys. A* **58** (2025) no. 17, 175202, [arXiv:2402.02984 \[quant-ph\]](#).

- [17] D. P. Sumner, "Graphs with 1-factors," *Proceedings of the American Mathematical Society* **42** (1974) no. 1, 8–12.
- [18] M. Las Vergnas, "A note on matchings in graphs," *Cahiers du Centre d'Études de Recherche Opérationnelle* **17** (1975) no. 2–3–4, 257–260. Colloque sur la Théorie des Graphes, Paris, 1974.